GROWTH AND ECOPHYSIOLOGY OF WIDE INTRASPECIFIC BALSAM POPLAR (*POPULUS BALSAMIFERA* L.) HYBRIDS

by

Natalie Marie Ryan

BSc. with Specialization in Environmental Biology, University of Alberta, 2009

A THESIS SUMBITTED IN PARTIAL FULFILLMENT OF THE REQUIREMENTS FOR THE DEGREE OF

MASTER OF SCIENCE

in

The Faculty of Graduate and Postdoctoral Studies

(Forestry)

The University of British Columbia

(Vancouver)

October 2015

Abstract

The widespread species *Populus balsamifera* L. exhibits large intra-specific variation in photosynthetic rates and phenology. Northern populations have a tendency towards higher photosynthetic carbon assimilation rates (A_n) than trees from the south. However, because bud set occurs earlier in northern trees they accomplish far less height growth than do southern trees. Assuming that there are no physiological constraints to combining high A_n and long growing season, the progeny of intra-specific crosses between northern and southern populations may accomplish more growth in one growing season than their parents (i.e., heterosis). High performing F_1s could be used for a variety of agroforestry projects. Full reciprocal crosses were conducted between individuals from two northern (N) and two southern (S) populations found at the extremes of the *P. balsamifera* range. Representative selections of progeny and parental material were planted in a greenhouse and in the field and characters including shoot elongation rate, photosynthetic rates, stomatal conductance (g_s), water-use efficiency (WUE) leaf mass per area (LMA), internal conductance (g_m) in a greenhouse and phenology in the field were evaluated. Although the F_1 families did not display any evidence of heterosis, photosynthetic rates and phenology were uncorrelated in the N×S families, suggesting an uncoupling of traits. Additionally, a number of individuals which possessed a combination of high growth potential and late growth cessation (bud set) were observed and could be useful for a variety of potential deployment areas. The high A_n in northern populations has been partially attributed to g_m, and appears to be a consequence of leaves with greater LMA, which have an increased mesophyll surface area available for carbon uptake. WUE was also correlated with LMA, suggesting that in facilitating CO_2 diffusion for carbon assimilation an increase in g_m over an increase in g_s provides a clear advantage in not promoting further water loss.

Preface

The study was conceived by Dr. Robert Guy and Dr. Raju Soolanayakanahally. Bill Schroeder, Dan Walker, and Garth Inouye were responsible for conducting the breeding protocols. The protocol for the A-C_i curve fitting method was devised by Dr. Raju Soolanayakanahally. The protocol for the extraction of the aqueous phase was devised by Dr. Robert Guy, in addition to advising on data interpretation and editing the thesis. Advice on data interpretation was also provided by Dr. Sally Aitken. Don Reynard provided technical support in the greenhouse and field. Melissa Mushanski, Félicia Corbeil, Vanessa Naish and Evan Dracup aided in the propagation, care and maintenance of plant material, and in the measurements undertaken in the greenhouse and field. I devised the field experiment, conducted gas exchange, height measurements, and phenological scoring, extraction of the aqueous phase and A-C_i curve fitting. I was also responsible for the data analysis and drafting the thesis.

Table of contents

List of Tables

List of figures

List of abbreviations

Abbreviation	Definition	Units
Δ	carbon isotope discrimination	‰
$\delta^{13}C$	carbon isotope abundance parameter	‰
A_{area}	photosynthetic rate per unit leaf area	µmol CO_2 m^{-2} s^{-1}
A_{mass}	photosynthetic rate per unit leaf mass	nmol CO_2 g^{-1} s^{-1}
A_n	net photosynthetic carbon assimilation rate	µmol CO_2 m^{-2} s^{-1}
AgCanBaP	Agriculture Canada Balsam Poplar collection	N/A
DBS	days to bud set	days
C_a	concentration of CO_2 in the air	µL L^{-1}
C_i	concentration of CO_2 at the evaporative surface inside the leaf	µL L^{-1}
g_s	stomatal conductance	µmol CO_2 m^{-2} s^{-1}
g_m	internal conductance	µmol CO_2 m^{-2} s^{-1}
J	rate of photosynthetic electron transport	µmol CO_2 m^{-2} s^{-1}
LMA	leaf-mass per area	mg cm^{-2}
N_{area}	nitrogen per unit leaf area	mmol N m^{-2}
N_{mass}	nitrogen per unit leaf mass	mmol N g^{-1}
N×N	north × north F1 cross	N/A
N×S	north × south F1 cross	N/A
PNUE	photosynthetic nitrogen-use efficiency	µmol CO_2 mol^{-1} N s^{-1}
R_d	day respiration	µmol CO_2 m^{-2} s^{-1}
RSE	rate of shoot elongation	cm day^{-1}
S×S	south × south F1 cross	N/A
S_{mes}/S	exposed surface area of mesophyll cells per unit leaf area	m^2 m^{-2}
TPU	triose phosphate use	µmol CO_2 m^{-2} s^{-1}
V_{cmax}	maximum carboxylation rate of Rubisco	µmol CO_2 m^{-2} s^{-1}
VPD	vapour pressure deficit	kPa
WUE	water-use efficiency	µmol CO_2 $mmol^{-1}$ H_2O

Acknowledgments

There are many people whose help and encouragement were essential for the completion of this thesis. First and foremost I would like to thank my supervisor Dr. Rob Guy. I will never be able to thank him enough for his unmeasurable patience in guiding me through this process. Thank you to the Faculty of Graduate Studies and the Faculty of Forestry for extra support during trying personal times. And to the members of the Guy Lab (Limin, Shofi, Athena, Lee, Linda, Mina, and Estefania) for providing such a supportive and collaborative lab experience.

I owe special thanks to all of my friends at the AAFC-AESB Shelterbelt Centre. Thank you to Félicia Corbeil, Evan Dracup, Melissa Mushanski, Vanessa Naish and Joanne MacKay for all the help and care they took in helping me with the research. Thank you also to Alisha Beler, Colin Billet, Erika Schuurmans, Kathy Ringdal, Meagan Tungate, Nikki Wirtz, Renee Howard, Sharon Hankey and Cassandra Knight for additional help in the field. Very special thanks to Don Reynard who was so generous in sharing his knowledge and time. And to Dr. Salim Silim whose excellent mentorship led me on the path to studying plant physiology and graduate studies.

I would also like to thank Dr. Raju Soolanayakanahally whose work provided me the framework for my study, as well as his un-ending support and advice. Thank you also to Dr. Sally Aitken for being part of my supervisory committee and for providing editorial services and advice.

I acknowledge the financial support of AAFC-AESB Shelterbelt Centre through the Student Research Affiliate Program. I would also like to acknowledge the financial support of Albert Environment and Sustainable Resource Development and an NSERC Discovery Grant both through Rob Guy.

Finally, with my whole heart, I would like to thank my parents, Kevin and Paulette Ryan, my extended family, and Mikkel Arnston. Without them all I would never have been able to make it this far.

For my parents and their unwavering love and support

CHAPTER 1. Literature review and thesis objectives

1.1 Introduction

Balsam poplar (*Populus balsamifera* L.) is a boreal and north temperate tree species with a large geographic range, from Alaska to Newfoundland and from Nunavut to Colorado (Figure 1.). Wide geographic distributions and access to the complete genome sequence of *Populus trichocarpa* Torr. & Gray (Tuskan et al. 2006) make species of the *Populus* genus ideal candidates for the study of the genetic basis of adaptive traits in trees. A collection of plant material from the range of *P. balsamifera* has been established at the Agriculture and Agri-Food Canada (AAFC) Shelterbelt Centre in Indian Head, Saskatchewan for use in such studies and for the purposes of conservation. The Agriculture Canada Balsam Poplar (AgCanBaP) collection contains material from 15 distinct genotypes each of 62 provenances (Figure 1.1).

In the past (1901-2013) the AAFC Shelterbelt Centre's Prairie Shelterbelt Program developed, produced, and deployed hardy and fast growing trees to Canadian Prairie farmers and landowners. These trees were used for a number of agro-forestry projects, mainly shelterbelts that protect crops, livestock and farm buildings. While the Prairie Shelterbelt Program is no longer operational, the replacement of existing, aging agroforestry projects will be necessary. Many hybrid poplar clones, which are ideal agroforestry trees due to their fast growth and hardy nature, have been developed at the Centre. Another approach with potential to meet the adaptive challenges of extreme Canadian climates is to take advantage of the genetic diversity of balsam poplar through breeding within the species.

1.2 Phylogeography of *Populus balsamifera*

As a consequence of the recurrent movements of the continental ice sheets during the Pleistocene, a restructuring and redistribution of populations in the northern hemisphere occurred during the twenty thousand years since the Last Glacial Maximum (Keller et al. 2010). During this time, North American and Eurasian (Iwasaki et al. 2012; Petit et al. 2003; Taberlet et al. 1998) forest trees migrated in waves out of refugia to recolonize their former geographical ranges, some within only a few hundred generations (Keller et al. 2011). During these range expansions, demographic events led to changes in genome-wide genetic diversity (Petit et al. 2003; Hewitt 2000; Talbert et al. 1998). Stochastic events led to strong genetic drift through allele surfing and founder effects resulting in gradients in allele frequency and population structure in these forest tree species (Hofer et al. 2009; Excoffier and Ray 2008).

Balsam poplar is one such forest tree which colonized the boreal and north temperate regions of North America that were once covered by the continental ice sheets (Williams et al 2004). In a study conducted by Keller et al. (2010), 412 SNP markers were developed to analyze how range expansion shaped the genetic diversity of balsam poplar. The study genotyped 474 individuals from 34 populations across the geographic range, and analyzed nucleotide diversity within and among populations. DNA sequence data and coalescent models complemented the set of SNP data and made it possible for the researchers to estimate historical population sizes and demography of the refugial population. Three demes differing in the magnitude of divergence from the ancestral allele frequencies were identified; a Northern deme (Alaska and Yukon), a large Central deme (western and central Canada), and an Eastern deme (Ontario, Quebec, Maritimes). Evidence from the SNP marker diversity and the coalescent models suggest that the

Central deme was the least differentiated from the refugial population and an asymmetrical migration away from the center towards the north and east had occurred.

1.3 Local adaptation of traits

Although the genetic diversity among and within populations of boreal tree species would likely have occurred initially as a result of stochastic sampling from the refugial population, expanding populations would have also encountered new selective pressures in novel environments (Keller et al. 2011). Environmental factors, such as temperature, photoperiod, and precipitation vary with latitude and altitude, and may have led to the establishment of selection gradients or clines in the direction of the migration (Keller et al. 2011). Therefore, colonizing species with large geographic ranges would be expected to show phenotypic variation in traits which reflect local adaptation to these novel environments (Keller et al. 2011). High intra-specific variation and clinal patterns in morphological and physiological traits of *P. balsamifera* and other species with large geographic ranges is well documented (McKown et al. 2014a; Soolanayakanahally et al. 2013; Soolanayakanahally et al. 2009; Gornall and Guy 2007; Chmura 2006; Arntz and Delph 2001; Benowicz et al. 2000; Poorter et al. 1999; Reich et al. 1999; Howe et al. 1999).

1.3.1 Phenological traits

For species with large geographic ranges in seasonal environments, the timing of traits related to growth and development are under strong local selection (Alberto et al. 2013; Savolainen et al. 2007; Howe et al. 2003). Phenology is the study of the timing of yearly events such as spring bud flush, growth cessation, autumn bud set and leaf senescence. The two major environmental cues which are primarily responsible for the induction of phenological traits are

temperature and photoperiod (day length). These environmental factors vary widely over a geographic range and therefore different optimal phenological phenotypes will be favoured in different parts of a species' geographical range.

In most trees, including poplar, the induction of bud flush is based mainly on seasonal changes in temperature and occurs when the 'minimum accumulative thermal time' reaches a critical level (heat sum) after dormancy is broken by chilling (Cooke et al. 2012). Clinal patterns in chilling requirements and heat sums have been reported in several forest tree species (Wuehlisch et al. 1995; Worrall 1983). In a study of 35 populations of balsam poplar grown in two common gardens (Vancouver, British Columbia (49.26°N, 123.25°W; elevation 82 m) and Indian Head, Saskatchewan (50.52°N, 103.68°W; elevation 605 m)), Soolanayakanahally et al. (2013) found date of bud flush and latitude of origin to be negatively correlated at both sites. The spring phenophase also occurred earlier and over a longer period of time in the coastal (Vancouver) common garden as compared to the continental (Indian Head) site, likely as a result of the differing spring temperature regimes (Soolanayakanahally et al. 2013).

While temperature is the primary cue for the induction of the spring phenophase, the dominant cue for the induction of summer and fall phenophases (height growth cessation, bud set, leaf senescence and leaf drop) in many temperate and boreal tree species is photoperiod, more specifically increasing night length (Rohde et al. 2011; Fracheboud et al. 2009). The critical photoperiod (the longest photoperiod required to cause a shift in phenology) in many forest tree species appears to increase with latitude of origin (Soolanayakanahally et al. 2013) and as a consequence, the date of bud set (Holliday et al. 2010; Ingvarsson et al. 2006; Hurme et al 1997; Wuehlisch et al. 1995; Worrall 1983; Morgenstern 1978; Heide 1974; Nienstaedt and Olson 1961) and leaf senescence (Soolanayakanahally et al. 2013; Rohde et al. 2011;

Fracheboud et al. 2009) show strong genetic differentiation across latitudinal clines (Soolanayakanahally et al. 2009; Aitken et al. 2008; Savolainen et al. 2007; Viherä-Aarnio et al. 2006; Howe et al. 2003; Howe et al. 1995; Junttila 1980). For example, northern (54°N) and southern ecotypes (34°N) of black cottonwood (*P. trichocarpa*) were evaluated in a study conducted by Howe et al. (1995). While short days in the greenhouse induced bud set in both ecotypes, northern ecotypes responded to a longer critical photoperiod than did the southern ecotypes. In addition, northern ecotypes were found to be more sensitive to photoperiod, and therefore the northern ecotypes required a shorter time to respond to photoperiod than the southern ecotypes.

1.3.2 Photosynthetic carbon assimilation rates

Local selection of intrinsic physiological characteristics such as photosynthetic carbon assimilation rates have also been observed in temperate and boreal tree species. Benowicz et al. (2000b) examined Sitka alder (*Alnus sinuata* Rydb) and paper birch (*Betula papyrifera* Marsh) from locations across British Columbia, Canada. When grown in the greenhouse, genotypes from locations with cooler winters in both species were observed to have higher photosynthetic rates. Latitudinal clines in photosynthetic carbon assimilation rates (*A*) in forest trees with large geographic ranges have also been observed. Gornall and Guy (2007) examined five provenances of black cottonwood along a latitudinal gradient and observed that *A* increased with increasing latitude of origin. A similar cline in photosynthetic carbon assimilation rates was also reported in the closely related species *P. balsamifera* (Soolanayakanahally et al. 2009).

1.4 Trade-off between intrinsic growth potential and phenology

In a preliminary study (data not included), gas exchange, height and diameter measurements were conducted on five genotypes of *P. balsamifera* from ten populations along a latitudinal gradient, growing in a common garden. Genotypes of northern provenances were observed to have higher photosynthetic carbon assimilation rates than those of southern provenances. The peak season rate of height and diameter growth in northern provenances of *P. balsamifera* was also much greater than in southern provenances. However, northern provenances accomplish much less height growth in one growing season than do southern provenances, and after multiple growing seasons the trees from the south are much taller than those from the north (Soolanayakanahally et al. 2013). Other studies have similarly found an inverse relationship between growth rate and photosynthesis in temperate trees (Benowicz et al. 2000a; Benowicz et al. 2000b; Benowicz et al. 2001; Gornall and Guy 2007). Soolanayakanahally et al. (2009) reported a greenhouse study in which northern provenances of *P. balsamifera* grown under long day photoperiods also had greater rates of height growth than did southern provenances. These findings suggest that higher intrinsic photosynthetic rates in northern provenances enhance height growth. Therefore, growth of trees at high latitudes does not appear to be limited by photosynthesis but rather a differing response to photoperiod, as compared to trees from lower latitudes (Soolanayakanahally et al. 2009). As stated before, apical growth cessation under short day conditions in northern provenances is in response to longer photoperiods than in southern provenances. This response to photoperiod means that growth cessation and bud set occur earlier in the year in trees from northern provenances than trees from southern provenances, which is reflected in their growth.

High photosynthetic carbon assimilation, early growth cessation, and early bud set are likely adaptive responses to a shorter growing season in the north (Soolanayakanahally et al. 2009, Gornall and Guy 2007; Viherä-Aarnio et al. 2006; Junttila 1982). Northern trees appear to be more conservative in their phenology likely due to the threat of an early frost late in the growing season. Northern provenances, therefore, appear to compensate for a shorter growing season with higher intrinsic photosynthetic rates that maximize growth during a short growing season (Gornall and Guy 2007). There is an apparent trade-off between photosynthetic carbon assimilation (*A*) and phenology. Trees from northern provenances have higher *A* but accomplish far less growth than do trees from southern provenances because of the early cessation of growth in northern genotypes. Gornall and Guy (2007) suggest that differences in photosynthate allocation to shoots/roots, photoinhibition, or oxidative stress may be responsible for this trade-off between physiological and phenological traits. More recently, in *P. trichocarpa*, McKown et al. (2014b) have provided genomic evidence for a north-south trade-off between carbon gain and disease resistance, mediated by stomatal patterning.

1.5 Stomatal conductance, water-use efficiency, photosynthetic nitrogen-use efficiency and internal conductance

The uptake of CO_2 from the atmosphere and the loss of water to the atmosphere through transpiration are both regulated by stomata. Stomatal conductance (g_s, mol H_2O m^{-2} s^{-1}) is measured as the rate of influx of CO_2, or efflux of water from the leaf, through the stomata and is directly related to the size of the stomatal aperture. However, the concentration gradient for the uptake of CO_2 is very small compared to the concentration gradient driving transpiration. Therefore, the challenge for terrestrial plants is to maximize their uptake of CO_2 while minimizing their water loss. Species with a high capacity for maximizing fixation while

minimizing transpiration are said to be water-use efficient. Water-use efficiency (WUE, μmol CO_2 $mmol^{-1}$ H_2O s^{-1}) at the leaf level is a measure of the amount of water lost during the fixation of CO_2 and can be expressed in two ways: as photosynthetic water-use efficiency (WUE_p; the ratio of the rates of photosynthesis (A) and transpiration (E)), or as intrinsic water-use efficiency (WUE_i; the ratio of photosynthesis (A) and stomatal conductance (g_s)). As g_s decreases WUE increases; however, a lower CO_2 intake is a result of a smaller stomatal aperture. As a consequence, the CO_2 concentrations at the chloroplast (C_c) and in the intercellular spaces (C_i) are low, and less of the total photosynthetic capacity is used. In addition to low photosynthetic rates, there is also a reduced photosynthetic nitrogen-use efficiency (PNUE, μmol CO_2 mol^{-1} N s^{-1}), the carbon gained per unit of leaf N. Therefore, under conditions of water stress WUE is maximized at the expense of PNUE. In contrast, in conditions of limited N availability, an increase in g_s is needed to increase PNUE at the expense of WUE. Therefore, a trade-off between WUE and PNUE is observed due to differences in C_i, as a result of variation in g_s under differing climate/nutrient conditions (Field et al. 1983). However, C_c is affected not only by g_s but also by the ease of diffusion of CO_2 from the sub-stomatal cavities to the site of carboxylation in the chloroplasts, also known as internal mesophyll conductance (g_m) (Warren and Adams 2006). Resistance to diffusion occurs as CO_2 moves from the sub-stomatal cavities through the intercellular air spaces of the mesophyll to the cell wall where it must enter the liquid phase to pass into the chloroplast. The resulting reduction in C_c imposes a limitation on photosynthesis, and consequently the relationship between WUE and PNUE is parallel in the same direction as g_m (Warren and Adams 2006). While the contribution of g_s to the photosynthetic rate is well understood, the role of g_m in the depletion of CO_2 at the site of carboxylation requires further elucidation. Genetic and environmentally induced inter-specific

variation in g_m has been documented in a number of studies (Rancourt et al. 2015, Muir et al. 2014, Warren and Adams 2006; Warren et al. 2003; Lauteri et al. 1997). Latitudinal variation in intrinsic photosynthetic rate in *P. balsamifera* has also been partially attributed to variation in internal mesophyll conductance (Soolanayakanahally et al. 2009). When comparing northern and southern *P. balsamifera* provenances, trees from northern provenances had higher g_m than did southern provenances. However, at present little is known about why internal mesophyll conductance is higher in trees at high latitudes. Warren (2008) suggested that trees growing at southern latitudes may invest in tougher leaves with thicker cell walls. It follows that a greater investment of nutrients and mass is required for leaves with long longevity for a long growing season. Thicker leaves or thicker cell walls would therefore increase the path length to the diffusion of CO_2, thereby decreasing internal mesophyll conductance.

1.6 Leaf mass area and internal mesophyll conductance

The leaf mass expressed per unit area, LMA, is often used as a proxy for leaf thickness in the literature, whereby thick leaves have a large mass for a given leaf area. In an analysis of species from across the globe, a general trend of increasing leaf longevity with increasing LMA has been observed (Wright et al. 2004). However, Soolanayakanahally et al. (2009) found that in *P. balsamifera* there was a strong correlation between latitude of origin and LMA. High LMA was found in populations from high latitudes, despite the comparatively short growing season and leaf longevity. The increased path length to diffusion of CO_2 that would be expected from leaves with a high LMA is contrary to the high g_m observed in northern populations. Therefore, another possibility for the variation in LMA observed in *P. balsamifera* may be variation in leaf anatomy.

The greatest resistance to the movement of CO_2 to the site of carboxylation appears to be in the liquid phase, rather than the gaseous phase in most species (Parkhurst and Mott 1990). The ease of diffusion of CO_2 in the liquid phase is negatively related to cell wall thickness and positively related to the surface area of mesophyll cells and/or chloroplasts exposed to the intercellular spaces (Scafaro et al. 2011, Terashima et al. 2011). LMA was found to be positively correlated with mesophyll thickness and surface area of mesophyll cells exposed to intercellular air spaces per unit leaf area (S_{mes}/S) in two evergreen species (Hanba et al. 1999). Internal mesophyll conductance (g_m) was also reported to be positively related to S_{mes}/S. Therefore, variation in surface area of mesophyll cells or some other leaf anatomical trait may be associated with the variation in g_m observed by Soolanayakanahally et al. (2009).

1.7 Heterosis

Natural hybridization between closely related species in nature has been well documented in the literature. Endogenous selection, due to meiotic, physiological or developmental abnormalities, may result in low survival or low hybrid fitness (Burke and Arnold 2001). However, a few, high performing recombinant hybrid genotypes may acquire novel adaptations which allow them to occupy new habitats (Arnold et al. 2008). Similarly, while the majority of hybrid genotypes perform poorly in experimental hybridizations, some hybrid genotypes may be found which perform better than their parents (Burke et al. 1998; Wang et al. 1997; Rieseberg et al. 1996). The phenomenon in which the offspring of hybridizations have biomass, growth rates and/or fitness greater than the mid-parent value (the average between the two parents) or the better parent is called hybrid vigour or heterosis (Sinha and Khanna 1975).

Hybrid vigour in experimental inter-specific hybrids has been well documented in the literature. For example, in a study in which *P. trichocarpa* from northern latitudes (44-49°N) and

P. deltoides from the southern latitudes (30-33°N) were hybridized, progeny with greater height and diameter growth, increased stem volume, and larger leaves with larger cells were observed (Ceulemans et al. 1992). The authors attributed the increase in biomass to the inheritance of leaves with more photosynthetically active tissue, which likely conferred greater photosynthetic and growth rates. Ceulemans et al. (1992) also found that the first generation (F1) hybrids had longer leaf area duration and therefore higher growth yields. Intra-specific hybridizations between geographically distant populations may also lead to heterosis (Harfouche et al. 2000; Schmidtling and Nelson 1996). Johnston et al. (2003) found greater tree volume, diameter, straightness and wind-firmness in inter-provenance hybrids of *Pinus caribaea* var. *hondurensis*.

Studies examining hybrid vigour in natural and experimental hybridizations provide conflicting evidence regarding the genetic basis of heterosis. Three main hypotheses have been presented, (1) dominance, (2) overdominance, and (3) epistasis. The dominance hypothesis suggests that progeny have increased fitness when recessive deleterious alleles of one parent are suppressed by the dominant alleles of the other parent (Davenport 1908). The over-dominance hypothesis attributes heterosis to heterozygotes having greater fitness over homozygotes at a single locus (East 1908, Shull 1908). Inbreeding within populations, due to the constraints of a finite population size, may result in recessive deleterious alleles becoming fixed (homozygotes). The over-dominance theory states that inbreeding depression is released through the complementation of different recessive alleles at a single locus in each of the parents, which provides the progeny (heterozygotes) with superior fitness. The hypothesis of epistasis proposes that heterosis is the result of the non-additive interaction between alleles at two or more quantitative trait loci (QTL) in hybrids (Fisher 1918). A favourable interaction between alleles produces novel gene combinations which result in highly fit hybrids. Evidence of over-

dominance (Stuber et al. 1992), epistasis (Cockerham and Zeng 1996), and dominance (Graham et al. 1997) in QTL studies of hybrid maize have all been reported in the literature. Similarly conflicting reports of the mechanism of heterosis in hybrid rice can also be found (Yu et al. 1997, Xiao et al. 1996). Therefore, generalizations about the genetic basis for heterosis within and across species are difficult to make.

Another, more current theory regarding the genetic basis of heterosis suggests that epigenetics may play a role in altering gene expression responsible for mediating metabolic pathways associated with growth and fitness (Chen 2013). Ni et al. (2009) found epigenetic modifications to circadian clock genes in *Arabidopsis* allotetraploids which increased the expression of downstream genes responsible for chlorophyll and starch content. The resulting altered metabolism lead to increased growth in these F1 hybrids compared to their parents *A. thaliana* and *A. arenosa*.

Heterosis is most often exhibited in the first generation (F1) with the increase in fitness appearing to break down through successive generations (Burke and Arnold 2001). Hybridizations between F1 genotypes (second generation, F2) which produce genotypes with greater fitness than the parental genotypes are likely due to the combination of alleles across non-interacting loci (Burke and Arnold 2001). The complementary action of parental alleles form new combinations that result in progeny with phenotypic traits that exceed those of their parents, much like heterosis (Riesberg 1999; Slatkin and Lande 1994). However, in this case, progeny with both greater and lower fitness than their parents are observed. The phenomenon in which hybridization results in extreme phenotypes is referred to as transgressive segregation.

The potential gain in fitness and productivity through the masking of recessive alleles relating to physiology, growth, and/or phenology in progeny or alternatively a release from

inbreeding depression through complementation makes hybridization a powerful tool for tree breeders.

1.8 Thesis objectives

As stated above, there appears to be a trade-off between photosynthetic carbon assimilation (A_n) and growth cessation in *P. balsamifera* in nature. Northern provenances have high A_n but respond to longer critical photoperiods and therefore accomplish less growth in a growing season than do trees from southern provenances. I set out to test the hypothesis that if no intrinsic physiological constraints exist which might prevent the combination of high *A* from the north and the longer growing period of the south, these traits could be combined in the progeny of intra-specific hybridizations between extreme northern and extreme southern provenances. Hybrid vigour may be observed in progeny with this combination of physiological and phenological traits and therefore the hybrids could potentially accomplish more growth in one growing season than either of their parents.

The relationship between intrinsic photosynthetic carbon assimilation rate, water-use efficiency, and internal mesophyll conductance is one that needs further exploration. Given that hybridization between genetically distant genotypes of the same species is likely to yield progeny with a high degree of variation in physiological and phenological traits, this may give an opportunity to further elucidate the relationship between A_n, WUE, g_s and g_m. By this same reasoning the relationship between LMA and A_n, WUE, g_s and g_m may also be explored.

Therefore, my objectives were as follows:

1. To compare the photosynthetic carbon assimilation rates, intrinsic growth rates and phenology of wide intra-specific hybrids with their parents.

2. To identify the progeny of intra-specific crosses that have high A_n and late growth cessation as candidates for further analysis.
3. To measure and examine trends in LMA of parents and progeny.
4. To estimate g_m in progeny and examine relationships with LMA, A_n, WUE, and g_s.

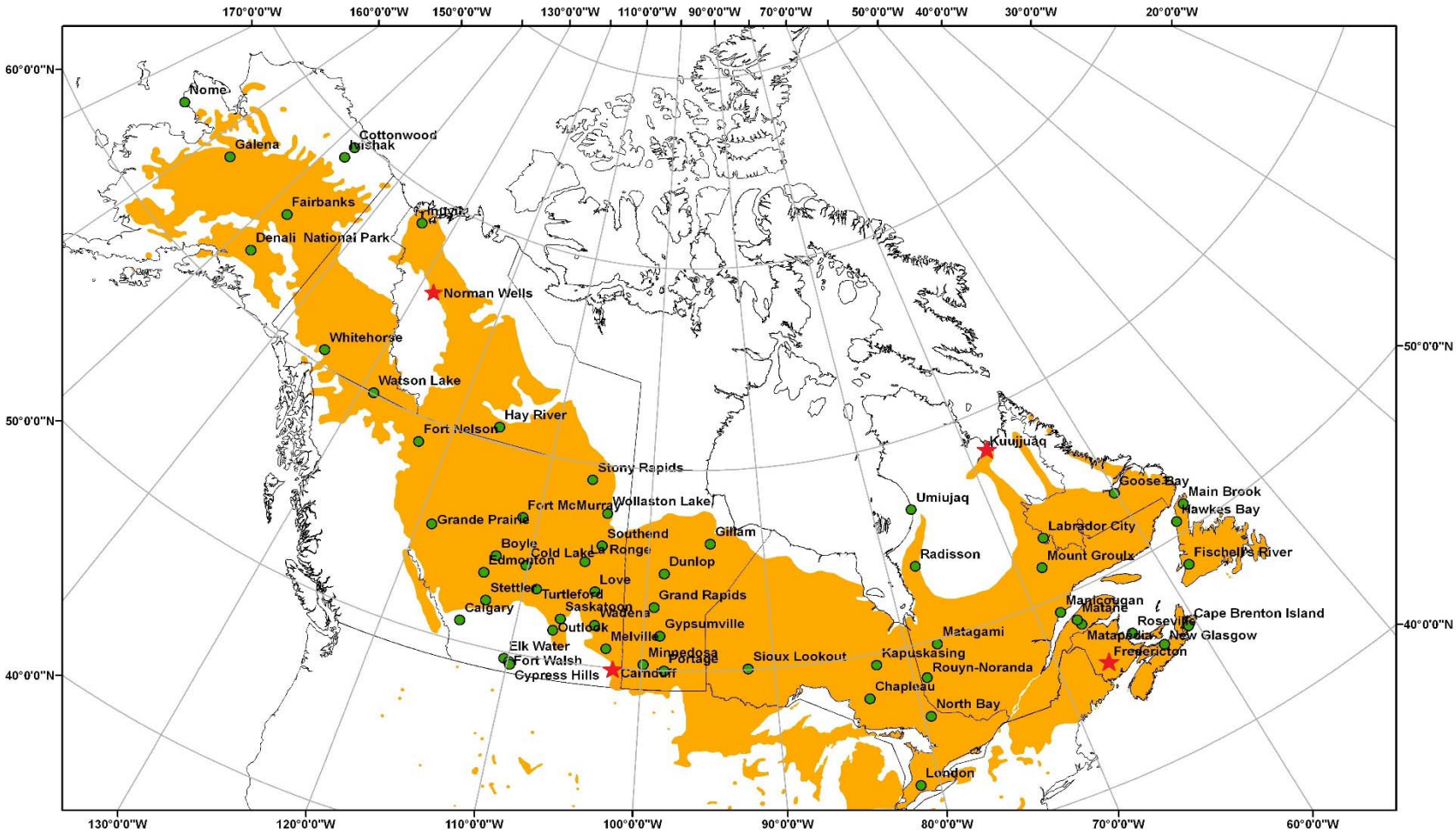

Figure 1.1 The geographic distribution of *Populus balsamifera* L. (area in orange) and the 62 provenances (green dots) represented in the Agriculture Canada Balsam Poplar (AgCanBaP) collection to date. Parental populations used in Chapters 2 and 3 (NWL and KUU in the north, and CAR and FRE in the south) are indicated by red stars.

CHAPTER 2. Uncoupling intrinsic growth potential and phenology in intra-specific hybrids of *Populus balsamifera* L.

2.1 Introduction

Large intra-specific variation and clinal patterns in morphological and physiological traits in temperate tree species with large geographic ranges are well documented (*Populus balsamifera* L. (Soolanayakanahally et al. 2013; Soolanayakanahally et al. 2009); *P. trichocarpa* Torr. & A. Gray (Gornall and Guy 2007; McKown et al. 2014a,b); *Betula papyrifera* Marsh. (Benowicz et al. 2001); *Alnus sinuata* Rydb. (Benowicz et al. 2000a); *Picea abies* L. (Junttila and Skaret 1990), *Pinus sylvestris* L. (Nilsson et al. 1995)). Photoperiod, one of the cues primarily responsible for the induction of phenological events, varies greatly across latitude and, consequently, strong latitudinal gradients in photoperiodic requirements have been widely reported (Aitken et al. 2008; Viherä-Aarnio et al. 2006; Hurme et al. 1997; Howe et al.1995; Wuehlisch et al. 1995; Worrall 1983). In a study conducted by Soolanayakanahally et al. (2009), bud set of 690 *P. balsamifera* (balsam poplar) genotypes grown in a common garden was negatively correlated with the latitude of origin. As a result, genotypes from northern latitudes set bud earlier than did genotypes from southern latitudes (Soolanayakanahally et al. 2009). Howe et al. (1995) reported that apical growth cessation under short day conditions occurred in response to a longer critical photoperiod in northern ecotypes of *P. trichocarpa* than in southern ecotypes. Northern ecotypes were also found to be more sensitive to photoperiod and consequently, required a shorter time to respond to photoperiod than did southern ecotypes (Howe et al. 1995).

When a selection of the same genotypes of *P. balsamifera* from the common garden established by Soolanayakanahally et al. (2009) were grown in a greenhouse under extended photoperiod to prevent bud set from occurring, height increment and photosynthetic rates were found to be positively correlated with latitude. Similar latitudinal gradients in growth and photosynthetic rates have been reported for other tree species with large geographic ranges (McKown et al. 2014a, Gornall and Guy 2007; Benowicz et al. 2001; Benowicz et al. 2000a; Benowicz et al. 2000b). However, trees from high latitudes of origin accomplished far less height growth than did those from low latitudes, a trend widely reported in common gardens of other tree species (e.g., *Picea abies* (Junttila and Skaret 1990), *Pinus sylvestris* (Nilsson et al. 1995), *P. trichocarpa* (Howe et al. 1995)). Given the smaller size of the northern genotypes in the common garden, the authors concluded that growth in the genotypes from northern provenances was not limited by photosynthetic rates but rather by the response to longer critical photoperiods resulting in a shorter growing season (Soolanayakanahally et al. 2009). Gornall and Guy (2007) suggested that northern provenances may have higher intrinsic photosynthetic rates and growth potential than southern provenances to compensate for the shorter growing season.

There is an apparent trade-off between photosynthetic carbon assimilation rates (A_n), growth, and phenology in *P. balsamifera*. Trees from northern provenances have higher A_n but accomplish far less growth than do trees from southern provenances because of the early cessation of growth in northern genotypes. Some cost to fitness (e.g., lower drought resistance, insect or disease resistance, shade tolerance) may have prevented the selection of genotypes with high A_n and late growth cessation in nature.

However, if no intrinsic physiological constraints exist which might prevent the combination of high A_n from the north and the longer growing period of the south, these traits could be combined through intra-specific hybridizations between northern and southern genotypes. The crossing of northern and southern genotypes of *P. balsamifera* could potentially produce hybrids which exhibit heterosis (hybrid vigour), the phenomenon in which the offspring of hybridizations have biomass, growth rates and/or fitness greater than the mid-parent value (the average between the two parents) or the better parent (Sinha and Khanna 1975). Heterotic genotypes combining the high A_n of the north and the late growth cessation of the south, may occur if recessive deleterious alleles fixed in the parental populations are masked or perhaps through the complementation of recessive parental alleles associated with physiological and phenological traits in the progeny (Burke et al. 2001). Through the combination of favourable traits the potential growth of the progeny of this hybridization could far exceed that of their parents.

Geographically distant genotypes of *P. balsamifera* from the Agriculture Canada Balsam Poplar (AgCanBaP) collection were used to test the hypothesis that intra-specific hybridizations of individuals from northern and southern populations yield progeny which exhibit greater growth than their parent populations through the combination of high A_n and late growth cessation. The north × south hybrids would be considered heterotic if they deviated from the mid-parent values that would be expected if simple genetic recombination was the outcome of the hybridization. Progeny which exhibit hybrid vigour in their growth may be valuable in the establishment of agroforestry projects which require fast growing genotypes.

2.2 Materials and methods

Parent material

The parental plant material used to conduct the intra-specific crosses was procured from the AgCanBaP collection (Soolanayakanahally et al. 2009). Genotypes from four provenances in the collection, two northern and two southern, were used (Fig 2.1). The northern provenances were Norman Wells, Northwest Territories (NWL; 65.23°N, 126.67°W) in the west and Kuujjuaq, Québec (KUU; 58.02°N, 68.65°W) in the east. The southern provenances were Carnduff, Saskatchewan (CAR; 49.18°N, 101.83°W) in the west and Fredericton, New Brunswick (FRE; 46.40°N, 67.25°W) in the east. These four provenances were chosen as they are from the extremes of the *P. balsamifera* range and therefore, are likely to be genetically distant.

Breeding

The intra-specific crosses were conducted in April 2009, in the greenhouse at the Agriculture and Agri-Food Canada, Agroforestry Development Centre in Indian Head, Saskatchewan. *P. balsamifera* branches with flower primordia from three female genotypes of each provenance were rooted in pots with a 3:1 mixture of Sunshine #2 (60% growing mix, 30% peat, 10% vermiculite) and Sunshine Peat Moss (100% peat) (Sun Gro Horticulture Canada, Seba Beach, AB) in a cold room by keeping the soil temperature at ~18°C. The three male branches were grown in a greenhouse in pots with water medium and, once anthers in male flowers matured, pollen from the male flowers was collected. For each provenance, the pollen from the three male genotypes was collected and mixed together (poly-blends). Upon rooting in cold room the females were

moved into greenhouse and the pollen were deposited using a paintbrush on the stigmas of receptive female flowers. All possible reciprocal crosses (intra- and inter-provenance) were conducted and are represented in Figure 2.1. Of the 48 crosses conducted, 41 produced offspring. Fully developed seeds were collected and the trichomes removed from the seed mechanically. Seeds were then germinated as families of hybrids on the above mixture of peat moss in Styroblock® Copperblock 77/170 mL containers.

In July 2009, 20 genotypes randomly selected from each family were transplanted into 2L pots with the above growing mixture. To the peat moss mixture 7 g dm^{-3} 18-6-8 Nutricote Total Controlled Release Fertilizer (Plant Products Co., ON, Canada) was added. Fifteen genotypes of each of the four parental provenances (from the AgCanBaP collection) were grown along with the hybrids as pseudo-parents. Pseudo-parents were used because plant material could not be propagated from the original parents. Rooted cuttings were grown in 965 mL plastic containers with the above mixture of peat moss and were later transplanted to 2L pots with the above mixture of peat moss and fertilizer.

The transplanted seedling (hybrids) and rooted cuttings (pseudo-parents) were grown in a greenhouse with natural light supplemented by fluorescent lamps to provide a photoperiod of 22 hours. The 15 hour day light in August in Indian Head (50° 34’ N/ 103° 40’ W) was extended to prevent bud set from occurring in the northern parents and hybrids who may exhibit a photoperiodic response similar to their northern parent. Day/night temperature in the greenhouse was 25/20°C, and daytime vapour pressure deficit (VPD) was 1.88 kPa. Seedlings were watered as needed and staked to ensure vertical growth and reduce self-shading. The seedlings were also given supplemental fertilizer (watered with a 200 ppm nitrogen solution made from 18-18-18 fertilizer (Plant

Products CO., ON, Canada)) after suspecting that the rate of height growth exceeded the rate of nutrient release from the controlled slow release fertilizer. Pots were fully randomized once a week to minimize any positional effects.

Nomenclature

Pseudo-parent populations were given the same three letter code used to designate the population in the AgCanBaP collection from which they were selected. For example, the pseudo-parent population from Kuujjuaq, QC is named KUU. Each F1 family was given a name of the following form: ♀*X*×♂*X*, where the first *X* represents the mother and the second *X* represents the father. The identity of the female parent is indicated by the first letter of the parent population (C (CAR), F (FRE), K (KUU), N (NWL)) and a number which denotes the identity of an individual mother. For example, ♀K4 is one mother from the KUU population which was used in the breeding of F1s. As the pollen from the three fathers in each parent population was mixed, only the first letter of the parent population represents the paternity of the family. For example, a father from the CAR population family will have a name which includes a ♂C element. Therefore, one of the three families with a KUU mother and a CAR father is named ♀K4×♂C.

Common garden establishment

In the last week of August the crosses and the pseudo-parents were moved to an outdoor shade house. In late October to early November, after bud set, leaf drop and the induction of dormancy, the trees were moved to a cold storage facility packed in thick polythene bags to prevent desiccation. In January 2010, stem cuttings from the dormant trees were

collected and stored in a -4°C freezer for future use. The remaining potted root systems were kept in cold storage until the following spring.

Early in May 2010 the potted rootstock was removed from cold storage and allowed to thaw out in the outdoor shade house. Prior to the initiation of spring bud burst, the rootstock was used in the establishment of a common garden at Indian Head (50.57°N, 103.67°W). Ten genotypes from each family and pseudo-parent, each represented by one transplanted rootstock, were planted in a group with 2.75m × 1m spacing and the families and pseudo-parents were then randomized within a block. A second randomized block with the remaining ten genotypes was established. The common garden was established to compare phenological traits between genotypes.

Greenhouse plants

The same genotypes grown in the field common garden were used to establish a greenhouse common garden to compare physiological and growth traits between genotypes. In early May 2010, the cuttings of the hybrids and their pseudo-parents were removed from the freezer and prepared for rooting. Cuttings with 2-3 buds were grown in 965 mL plastic containers with the same peat moss mixture used for the seedlings grown in 2009. Ramets were grown in a greenhouse under the same environmental conditions as stated above. A completely randomized single-tree plot design was used in the greenhouse, and trees were fully randomized each week, for the duration of the study, to reduce any positional effects. The trees were then transplanted into 2 L pots with 7 g dm^{-3} 18-6-8 Nutricote Total Controlled Release Fertilizer (Plant Products Co. Ltd., Brampton, ON) added to the same peat moss mixture 45 days after rooting.

Height measurements

Height measurements of greenhouse plants were taken over six weeks which began following the transplanting of these trees into larger containers. Height in centimeters (cm) was measured as the length of the stem from the top of the peat moss to the base of the apical plumule. The height of each genotype was plotted against time to determine the shape of each curve. The linear portion of the curve was identified as the period of maximal growth with the slope of the line equal to the rate of shoot elongation (RSE; cm day^{-1}).

Steady-state gas exchange measurements

An infra-red gas analyzer (LC Pro+, Analytical Development Co. Ltd., Hoddesdon, UK) was used to measure net photosynthetic carbon assimilation (A_n) in trees grow in the greenhouse. Measurements were made on the third fully expanded, mature leaf from the apical plumule of each ramet 75 days after rooting. The measurements were conducted during the part of the day when maximum photosynthesis occurs (0900- 1300 h) as determined by analyzing the diurnal pattern of photosynthesis (data not shown). The CO_2 of the incoming air was maintained between 380 and 400 $\mu L\ L^{-1}$, the temperature in the chamber was maintained at approximately 25°C with a VPD of 1.88 kPa. A mixed red and blue LED unit mounted on top of the cuvette provided a saturating PPFD of 1131 $\mu mol\ m^{-2}\ s^{-1}$.

Phenological observations

Spring and autumn (2011) phenology was monitored in the outdoor common garden. Observations were recorded two times a week by the same personnel. A scale of 0 to 3

was used to describe the developmental stages of the terminal buds during spring bud burst (0= dormant bud, 1= swollen bud with visible green tips, 2= bud flush, 3= leaf emergence with visible petioles). The date leaf emergence occurred was considered to be the first day of green-cover. Autumn bud set was recorded as the date the terminal bud and the bud scales became fully developed. The number of days between leaf emergence and the formation of bud scales was termed 'days to bud set' (DBS).

Statistics

All statistical analyses used SigmaPlot 13.0 (Systat 2014). One way analyses of variance (ANOVAs) of A_n and RSE for the pseudo-parent populations and the 41 families of crosses were performed. The Holm-Šidák method (t-statistic) was used for multiple comparisons (Holm 1977). A separate ANOVA on Ranks was performed on the DBS of the F1s and pseudo-parents followed by pairwise multiple comparisons using Dunn's method (q-statistic) (Dunn 1964). Pearson's correlations were performed between RSE, A_n and DBS of the F_1s. A Chi-squared test was used on the top ten high performing individuals to check for differences in frequency from a random distribution among within-population, N×N, S×S, and N×S groups of crosses.

2.3 Results

Pseudo-parent populations

During the period of maximal growth in the greenhouse common garden, there was no significant difference in the net rate of carbon assimilation between the pseudo-parents from different populations (Fig. 2.2.A). However, the rate of shoot elongation (RSE) in the NWL pseudo-parent population was significantly greater than that of the

other northern pseudo-parent population, KUU ($q_{(3)}$= 3.502, P<0.05) and the two southern pseudo-parent populations, CAR ($q_{(3)}$= 2.905, P<0.05) and FRE ($q_{(3)}$= 4.269, P<0.05) (Fig. 2.2.B). Similarly, significant differences among these populations in the number of days to bud set of trees when grown in the field. The NWL pseudo-parents had significantly fewer days to bud set as compared to KUU ($q_{(3)}$= 3.379, P<0.05), CAR ($q_{(3)}$= 4.549, P<0.05), and FRE ($q_{(3)}$= 4.776, P<0.05) (Fig. 2.2.C). Additionally, the ranking in the mean RSE observed in the pseudo-parent populations grown in the greenhouse was opposite to that of mean DBS of pseudo-parent populations grown in the field. While northern pseudo-parent populations had high mean RSE and short mean DBS, southern pseudo-parent populations had low mean RSE and long mean DBS.

Patterns across all F_1 families

A positive, but weak and potentially curvilinear correlation between photosynthetic rate (A_n) and the rate of shoot elongation (RSE) was observed across all F_1 families combined (r = 0.330, P < 0.001) (Fig. 2.3). This correlation persisted when only the north×south (N×S) F_1 families were considered (r = 0.260, P < 0.001). A much weaker, significant negative correlation between RSE and the number of days to bud set (DBS) was also observed across all the F1s (r = 0.195, P < 0.001) (Fig.2.4), but did not persist in the N×S crosses considered alone (r = 0.046, P = 0.440). Days to bud set and A_n were not significantly correlated with each other in either case.

Within-population crosses

The variation in A_n (Fig. 2.5) and RSE (Fig. 2.6) as displayed by the range of each box plot, of the pseudo-parent populations and that of the progeny of within-population crosses, was greater than the variation observed in DBS (Fig. 2.7). Collectively, the variation in A_n and RSE of the progeny of within-population crosses between individuals from CAR, FRE and NWL appeared greater than that of their pseudo-parent populations (not tested). Differences in the variation in DBS between pseudo-parent populations and crosses were not apparent, nor was there any difference in variation between KUU and the within-population crosses for any of the three measured characteristics.

North × north and south × south crosses

As with the pseudo-parent populations and the within-population crosses, there were no significant differences in A_n between the north × north (N×N) or south × south (S×S) crosses and their pseudo-parents (Fig. 2.8.A and Fig. 2.8.B). The NWL pseudo-parent had significantly greater rates of shoot elongation than all three of the N×N families (Fig. 2.8.D). The ♀C3×♂F ($t_{(7)} = 4.465$, $P < 0.001$) and ♀C4×♂F ($t_{(7)} = 3.594$, $P = 0.014$) families had RSE that more closely resembled those of the FRE pseudo-parent, as the RSE was significantly lower than for the CAR pseudo-parent (Fig. 2.8.C). In the N×N crosses, the low DBS for the ♀K4×♂N ($q_{(5)} = 4.149$, $P < 0.05$) and ♀K5×♂N ($q_{(5)} = 4.572$, $P < 0.05$) families was more like the NWL than the KUU pseudo-parents (Fig. 2.8.F). Conversely, the ♀N6×♂K ($q_{(5)} = 3.836$, $P < 0.05$) and ♀K6×♂N ($q_{(5)} = 3.249$, $P < 0.05$) families were more like the KUU pseudo-parents, with significantly more DBS than the NWL pseudo-parents (Fig. 2.8.F). Three of the S×S crosses had significantly fewer

DBS than FRE, ♀C3×♂F ($q_{(7)} = 4.196$, $P < 0.05$), ♀C4×♂F ($q_{(7)} = 3.142$, $P < 0.05$), and ♀F10×♂C ($q_{(7)} = 3.420$, $P < 0.05$), while only ♀F11×♂C ($q_{(7)} = 3.647$, $P < 0.05$) had greater DBS than CAR (Fig. 2.8.E).

North × south population crosses

Overall, the progeny of N×S population crosses seemed to have greater variation in assimilation rates than their pseudo-parents (Fig. 2.9), but no significant difference in A_n between the N×S and pseudo-parents was found. Similarly, the variation in RSE appeared greater for the N×S crosses than for their pseudo-parents (Fig. 2.10). However, the RSE of the NWL population was significantly greater than five of the six FRE×NWL cross families and all four of the CAR×NWL cross families (Fig. 2.10, Table 3.1). Additionally, the RSE of the progeny of crosses between KUU and both southern pseudo-parent populations, most closely resembled the RSE of the KUU pseudo-parent. Many of these N×S cross families included individuals with higher rates of shoot elongation than either of their pseudo-parent populations (Fig. 2.10, Table 3.1). However, the majority of the individuals (those within the inter-quartile range) in these cross families were within the ranges of the pseudo-parent populations (Fig. 2.10).

Overall, the variation in DBS of both pseudo-parents and the corresponding N×S families appeared to be much lower than the variation observed in A_n and RSE between pseudo-parents and crosses (Fig. 2.11). In addition, the variation in DBS in the majority of N×S families did not appear to be greater than the variation observed in the pseudo-parent populations (Fig. 2.11). The DBS of the southern pseudo-parent populations was significantly greater than in 10 of the 22 N×S families (Fig. 2.11, Table 3.1). Also, the

DBS of the NWL pseudo-parent population was significantly lower than for 5 of the 6 progeny of the FRE×NWL crosses and 3 of the 4 CAR×NWL crosses (Fig. 2.11, Table 3.1). Similarly to RSE, although the DBS of some individuals is larger or smaller than one or the other pseudo-parent population, the inter-quartile range of the N×S families falls between the ranges of the pseudo-parent populations.

2.4 Discussion

Trait variation in pseudo-parents

The analysis of A_n, RSE, and DBS of the pseudo-parent populations was only partly consistent with the trade-offs among photosynthetic rate, growth potential and phenology of northern and southern genotypes of *P. balsamifera* reported by Soolanayakanahally et al. (2009). The most latitudinally extreme populations, NWL and FRE, behaved as expected in that bud set occurred earlier and RSE, under long day conditions, was greater in the former than in the latter (Fig. 2.2). However, no differences in assimilation rates among the four pseudo-parent populations were observed. Regardless of latitude of origin, in all three traits there appears to be large variation among and within provenances that can obscure the broad-scale geographic patterns seen across larger numbers of populations. Trends observed by Soolanayakanahally et al. (2009) were based on the analysis of 21 populations. Nonetheless, KUU and FRE had the highest and lowest rates of net carbon assimilation, respectively, in that study. They also had distinctly different RSE. Failure to find some of these same differences in the present study may be partly due to the low number of genotypes sampled representing the FRE population (n= 4 to 6).

Trait correlations across F_1 offspring

A key objective of the present work was to determine whether apparent trade-offs between A_n, growth, and phenology could be broken through wide intraspecific crosses. There were weak correlations between RSE and both A_n and DBS in the combined analysis across all F_1 families (Figs 2.3 and 2.4), but only the former correlation persisted when crosses between dissimilar latitudes were considered. Crosses conducted within populations, or indeed between populations from more similar latitudes (i.e., N×N and S×S), would not be expected to remove any geographic association between co-varying traits, such as RSE and DBS. On the other hand, it's not surprising that A_n and RSE should remain correlated across just the N×S F_1 families, as growth rate must at some level determine (or be determined by) the rate of photosynthesis. The absence of any relationship between RSE and DBS or A_n and DBS in the in the N×S crosses suggests that there are no barriers to combining superior performance in these traits.

Carbon assimilation and shoot elongation

Although the equal variance assumption was either met or, because of lack of normality, could not be tested in all ANOVAs comparing F_1 families with their pseudo-parents, variation in A_n and RSE appeared to be greatest in families resulting from between, rather than within, population crosses, especially if considered collectively (compare Figs. 2.8, 2.9, 2.10 and 2.11, with 2.5, 2.6 and 2.7). Higher variance in reciprocal crosses between disparate provenances might be expected given that phenotypic variation in traits between geographically distant populations exist and reflect local adaptation to very different environments.

Several of the crosses between provenances generated a few individuals with extreme phenotypes (outliers) for A_n and RSE; in particular, high A_n was seen in individuals resulting from between northern and southern genotypes (Fig. 2.9). However, only a few extreme phenotypes exist and most families did not differ from one or both pseudo-parents, or were intermediate to them. Due to a larger sample size, a greater number of outliers in the N×S crosses would be expected by chance as compared to the pseudo-parent populations. Therefore, recombination rather than heterosis appears to be the mechanism responsible for the combination of high A_n and RSE in some of the F_1s. Alternatively, the high performing genotypes may be a result of complementation of recessive deleterious alleles, which could have become fixed in parent populations through genetic drift at range margins. This would be most evident in hybridizations between populations with low genetic diversity. An exploration of the amount of genetic diversity within each of the pseudo-parent populations as well as other populations in the AgCanBaP collection may reveal potential crosses between *P. balsamifera* populations that are more likely to produce heterotic progeny.

Although heterosis in the physiological traits of the N×S crosses was not apparent, the outliers whose carbon assimilation and shoot elongation rates exceed the maximum rates of their northern parent may be ideal individuals for further examination. Additionally, these individuals could be used to examine the potential for transgressive segregation in physiological and phenological traits in an F_2 generation. The RSE of outliers in the majority of the families of the FRE×KUU and CAR×KUU hybridizations exceeded the maximum RSE of the KUU (northern) pseudo-parent population. Outliers in A_n in 14 of the 22 families of N×S crosses also exceeded the northern pseudo-parent

population. The individuals that were outliers in the RSE were not generally the same individuals that were outliers in A_n, although four N×S families had outliers for both traits (♀F10×♂K, ♀K5×♂F, ♀K4×♂C, and ♀C4×♂K).

Growth cessation in hybrid families

In comparison to A_n and RSE, the lower apparent variation in DBS in the pseudo-parents (and relative to the sum of their respective F_1s), is consistent with reports in other tree species of higher among-population and lower within-population genetic variation in fall phenological traits than in growth traits (Alberto et al. 2013; Aitken et al. 2008, Howe et al. 2003). These findings are supported by a study from Olson et al. (2013) which reported high broad-sense heritability ($H^2 > 0.5$) of bud flush and bud set in *P. balsamifera* genotypes from across the species range.

Similarly to A_n and RSE, the mean DBS and most of the individual variation in DBS did not deviate from the mid-parent expectation for genetic recombination (Fig. 2.11). However, while some individuals with extreme phenotypes (outliers) were observed, none of these genotypes exhibited growth cessation later than or nearly as late as the southern pseudo-parent genotypes, particularly for the N×S crosses with FRE. The lack of evidence of segregating genetic variance in bud set in the intra-specific hybrids suggests that complex gene interactions may be responsible for the latitudinal cline in bud set observed in forest tree species. The circadian clock *CO*/*FT* regulatory model has been identified as being involved in the timing of fall phenological events in several forest tree species (Böhlenius et al. 2006). Latitudinal clines in single nucleotide polymorphisms (SNPs) of the circadian clock genes *Gigantea* and *FTL2* associated with growth

cessation, as well as a latitudinal cline in gene expression of *FTL*2, have been reported in *Picea abies* and *P. obovata* (Chen et al. 2014). Wang et al. (2014) also reported a latitudinal cline in the differential expression of many of the genes in the *CO*/*FT* regulatory model throughout the stages of the autumn phenophase of *P. balsamifera*. In a study of four F1 families of inter- and intra-specific hybrids of *Populus* species, Rohde et al. (2011) found that QTL (quantitative trait loci) associated with bud set could be detected in 6 regions of the genome which were conserved across all four families. Additionally, in a genome-wide association study of *P. trichocarpa*, 240 genes were found to be associated with phenological traits, particularly with date of bud set (McKown et al. 2014a).

Gender

Within the N×S crosses, there were very few differences among families with parents from the same combination of provenances, regardless of which parent is from the north or south. The only differences observed among families was in the rate of shoot elongation in the ♀F3×♂N family, which was found to be significantly lower than that of ♀N2×♂F, ♀N3×♂F, and ♀N6×♂F families (Fig. 2.10.A.). It appears as though the higher growth rates observed in the NWL population (Fig. 2.2.A) are conferred to the offspring when the mothers and not the fathers are from NWL. However, as the potential influence of gender has only been observed in one group of cross families, and only for the RSE, it seems unlikely that gender plays a significant role in determining the A_n, RSE or DBS of the N×S crosses.

Selection of candidate progeny

As the mean trait values of A_n, RSE, and DBS did not exceed that of the pseudo-parent populations in any of the F_1 families, it can be concluded that heterotic genotypes were not produced from the intra-specific hybridization of latitudinally distant populations. However, A_n and DBS were found to be uncorrelated in the N×S families, which suggests that intrinsic growth potential and phenology can be uncoupled. Multiple individuals exhibiting a combination of high A_n, RSE, and DBS were observed. Of the top ten individuals which had the highest values for all the three characters measured, five individuals were from N×S cross families (♀N2×♂F-8, ♀N2×♂F-14, ♀N3×♂F-10, ♀F10×♂K-9, ♀F11×♂K-8). The remaining individuals in the top ten were from latitudinally distant S×S cross families (♀F3×♂C-3, ♀F10×♂C-10, ♀F11×♂C-18, ♀F11×♂C-19) and one from a within-population cross family (♀C4×♂C-12). However, the number of high performing individuals within each group (within-population, N×N, S×S, and N×S) did not differ from what would be expected by chance ($X^2_{(3)} = 5.4101$, n.s.). All the same, these high performing genotypes could be considered candidates for further exploration.

Candidate genotypes which exhibit high intrinsic growth rates similar to that of northern genotypes, and the late growth cessation of southern genotypes of *P. balsamifera*, should produce faster growing trees in the field at southern latitudes. Fast-growing trees would be ideal for the establishment of agroforestry practices, such as shelterbelts, silvo-pastures, riparian buffers and/or alley-cropping, which rely on the quick establishment of trees to protect farm buildings, crops and animals from the

elements such as, snow, winds, soil erosion and surface water run-off. Additionally, depending on the chosen geographical location of an agroforestry project, an individual with high intrinsic growth potential, with a DBS which matches the expected fall phenological response to the photoperiod of the local environment, could be selected and made available to landowners. Trees with high intrinsic growth potential may also yield greater overall biomass which could be ideal for the production of biofuels.

2.5 Conclusion

The objective of this study was to attempt to break the apparent trade-offs between intrinsic growth potential (A_n and RSE) and phenology (DBS) in *P. balsamifera* through the crossing of geographically distant genotypes. Uncoupling of these traits appears to have been accomplished in the N×S cross families as A_n and DBS were uncorrelated. While no evidence for heterosis was observed, the apparent large variation in traits across F_1 families included a number of individuals with a combination of high A_n, RSE and DBS. With further exploration of total growth of these select genotypes in the field, these potentially fast growing trees could be ideal for future agroforestry projects.

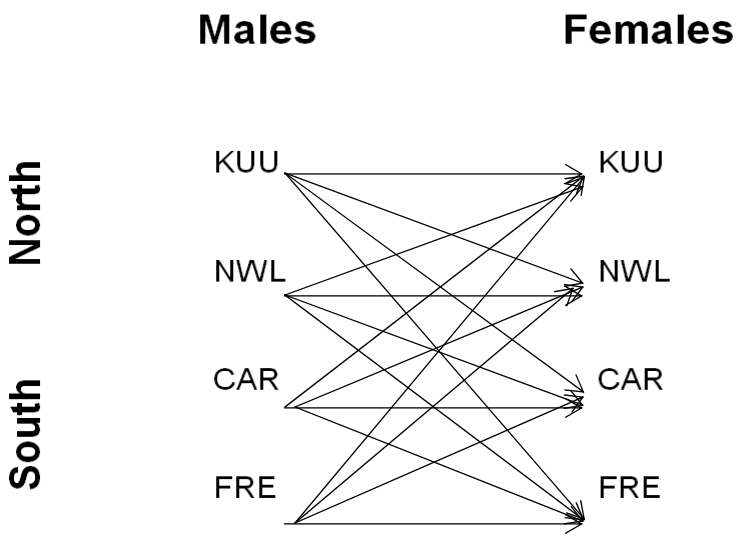

Figure 2.1 Breeding pattern used for all reciprocal crosses (within population, N×N, S×S, and N×S) performed.

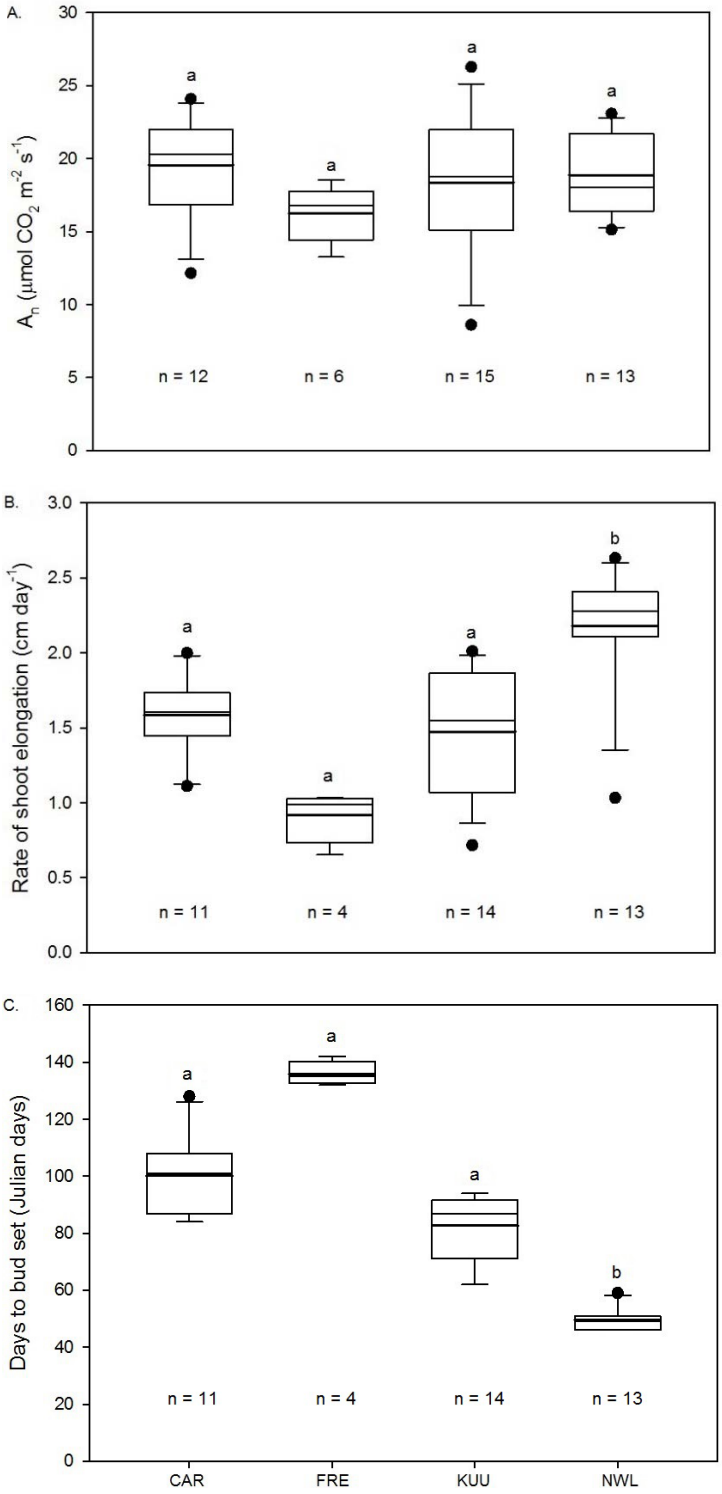

Figure 2.2 Box plots representing (A) photosynthetic rates (A_n), (B) rates of shoot elongation (RSE), and (C) number of days to bud set (DBS) of the pseudo-parents. Median = thin line; 3rd quartile (75th percentile) above, 2nd quartile (50th percentile) below, mean = thick line, outliers = circles, whiskers = 90th percentile, above, and 10th percentile, below.

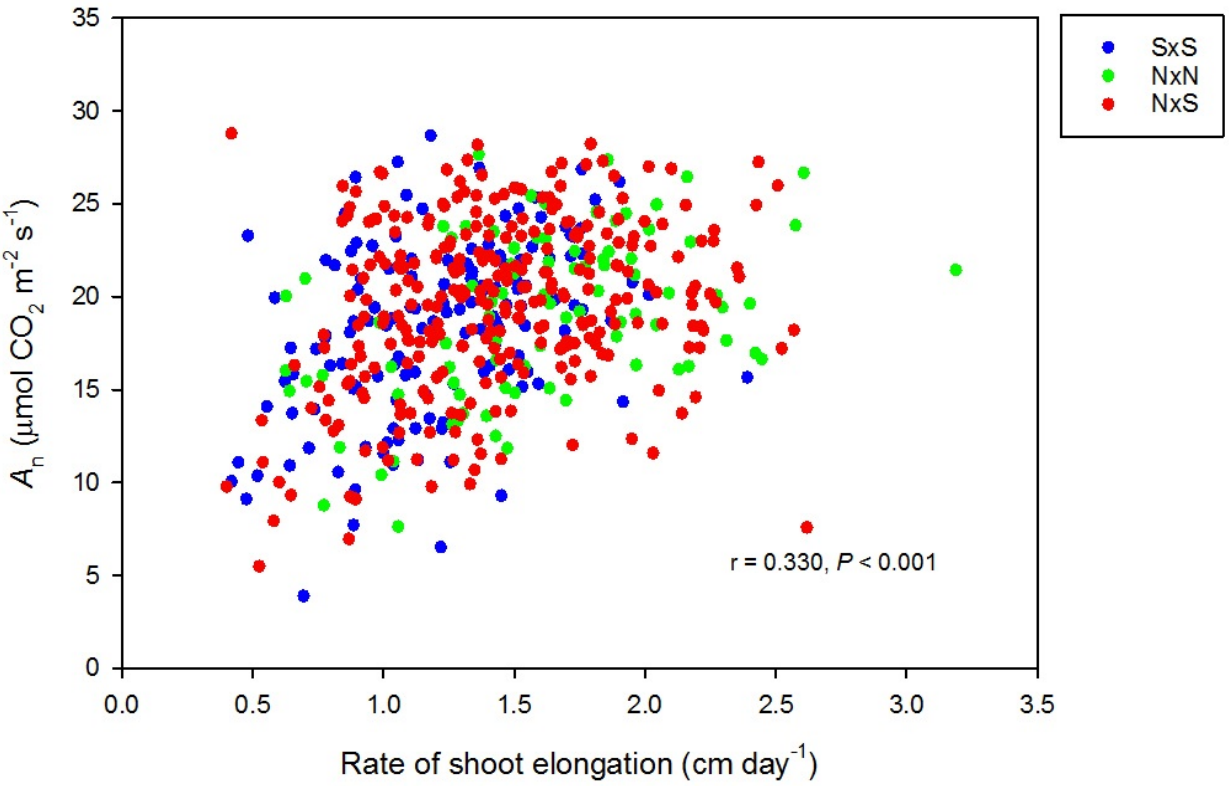

Figure 2.3. The relationship between the photosynthetic rate (A_n) and the rate of shoot elongation (RSE) of the F_1s of within population, north × north (N×N) and south × south (S×S) crosses, and north × south (N×S) crosses.

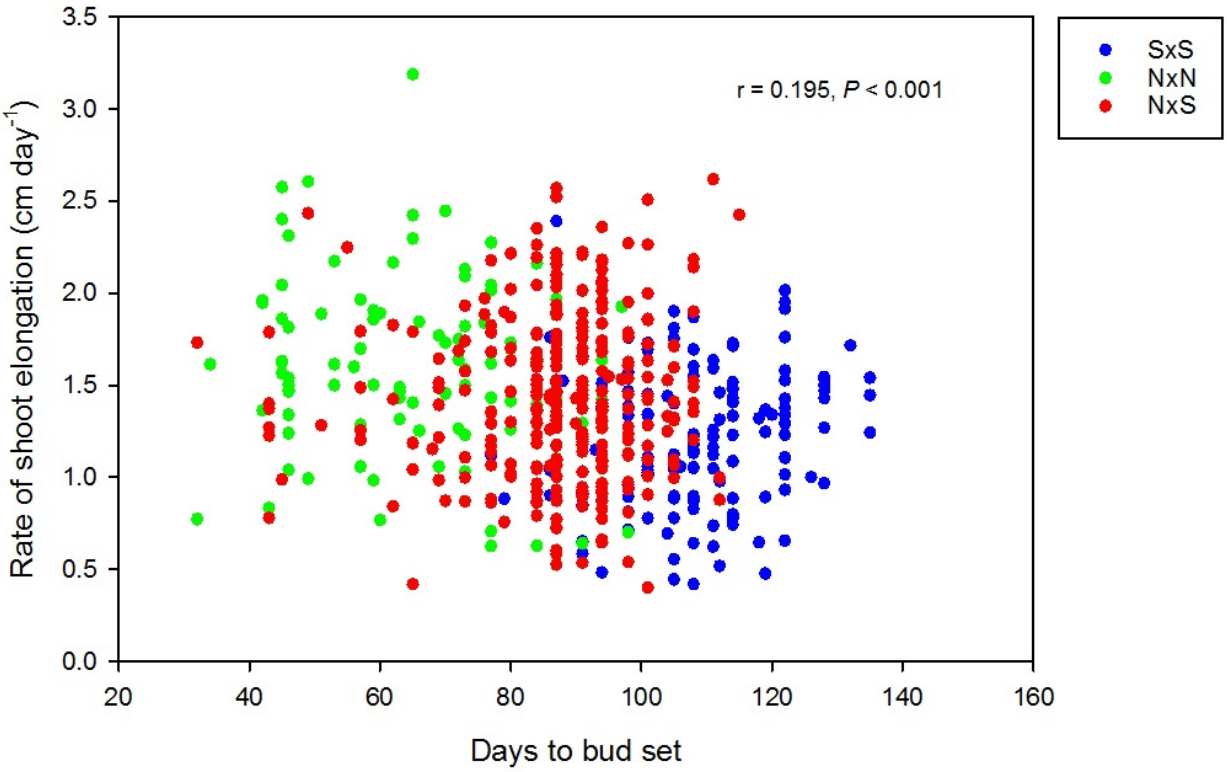

Figure 2.4. The relationship between the rate of shoot elongation (RSE) and the days to bud set (DBS) of the F_1s of within population, north × north (N×N), and south × south (S×S) crosses (open circles), and north × south (N×S) crosses (red circles).

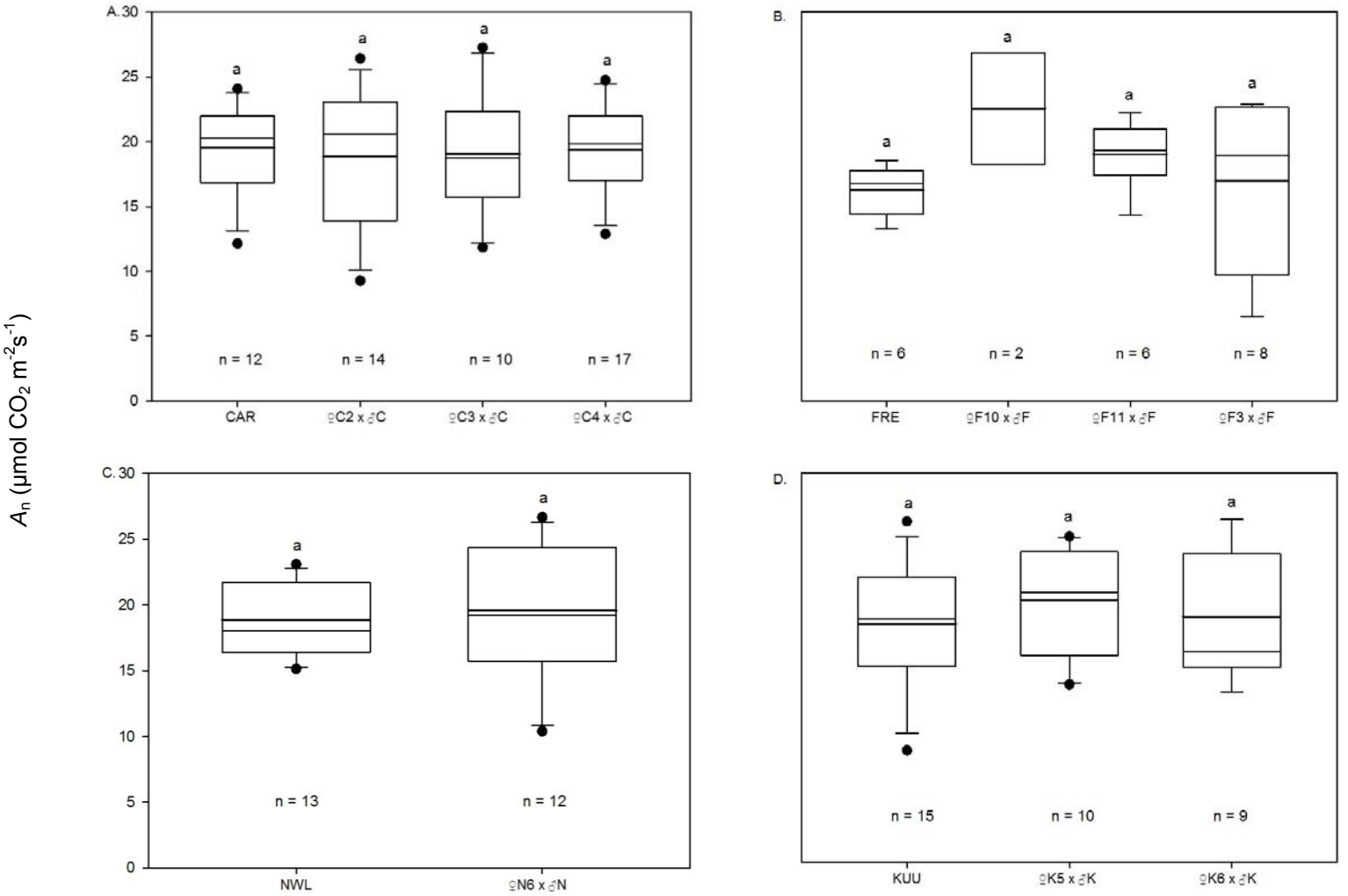

Figure 2.5 Box plots representing the net rate of carbon assimilation (A_n) of the pseudo-parents and the families of within population crosses. Median = thin line; quartile (75th percentile) above, 2nd quartile (50th percentile) below mean = thick line, outliers = circles, whiskers = 90th percentile, above, and 10th percentile, below.

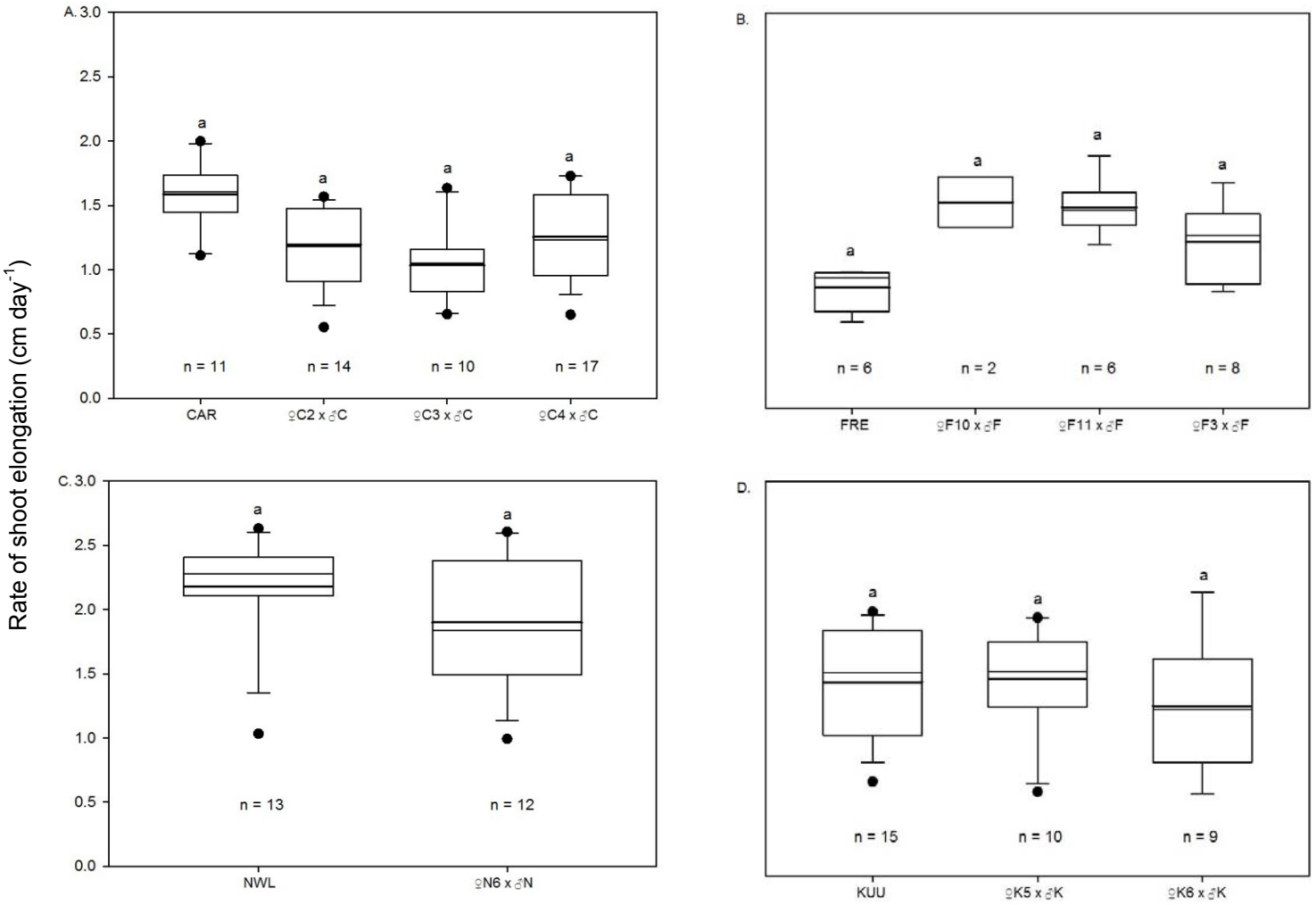

Figure 2.6 Box plots representing the rate of shoot elongation (RSE) of the pseudo-parents and the families of within population crosses. Median = thin line; quartile (75^{th} percentile) above, 2^{nd} quartile (50^{th} percentile) below, mean = thick line, outliers = circles, whiskers = 90^{th} percentile, above, and 10^{th} percentile, below.

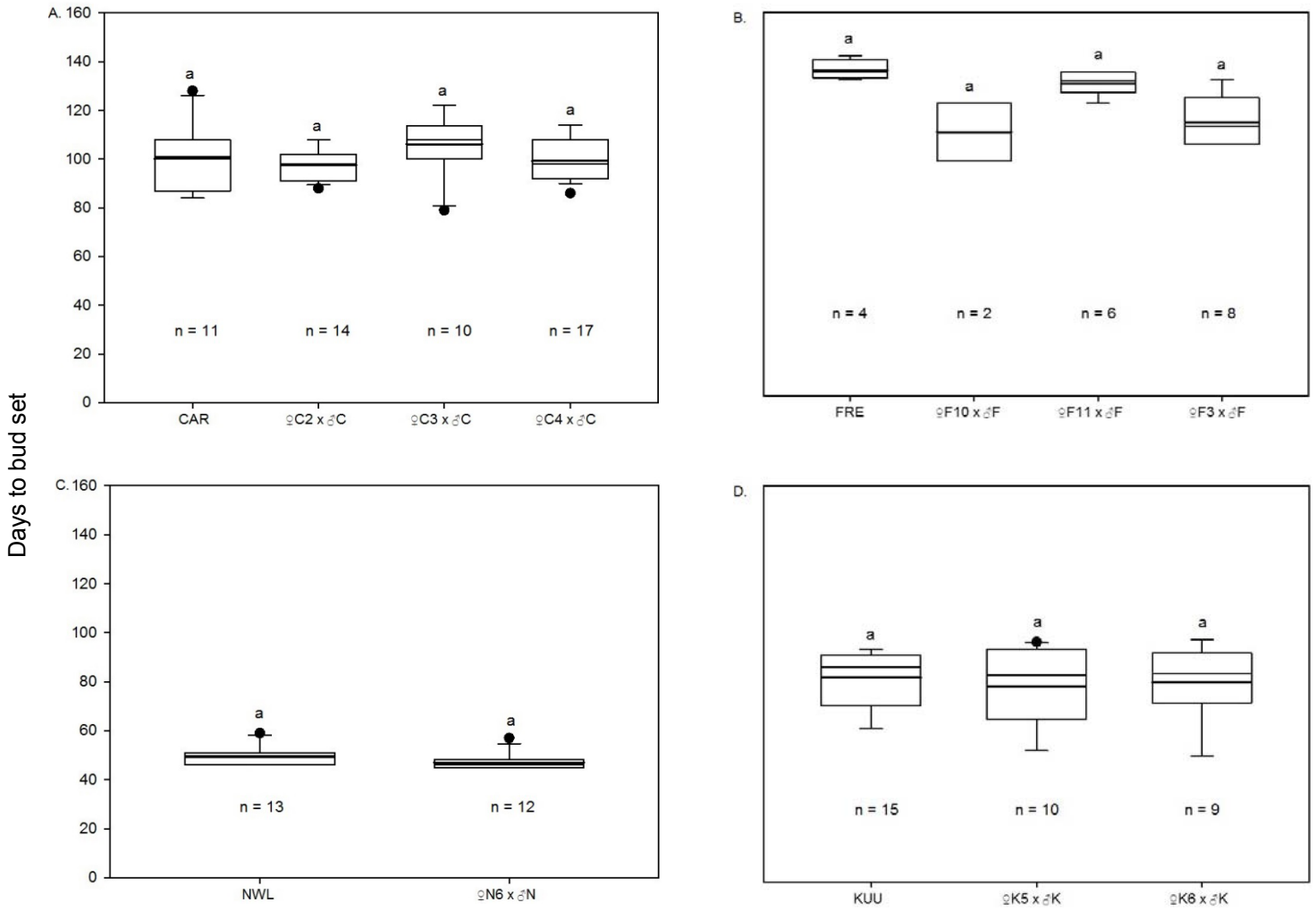

Figure 2.7 Box plots representing the number of days to bud set (DBS) of the pseudo-parents and the families of within population crosses. Median = thin line; quartile (75th percentile) above, 2nd quartile (50th percentile) below mean = thick line, outliers = circles, whiskers = 90th percentile, above, and 10th percentile, below.

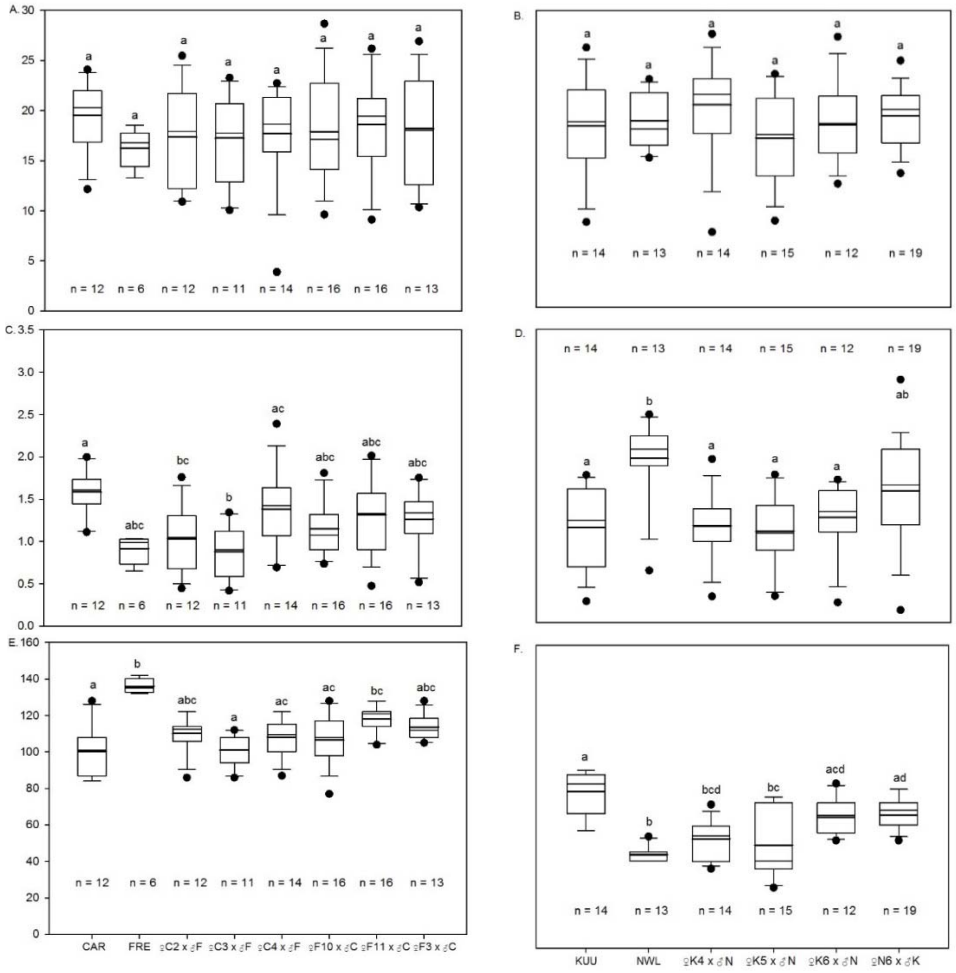

Figure 2.8 Box plots representing the (A, B) photosynthetic rates (A_n), (C, D) rates of shoot elongation (RSE), and (E, F) the number of days to bud set of the pseudo-parents and the families of south × south (S×S) and north × north crosses (N×N). Median = thin line; quartile (75th percentile) above, 2nd quartile (50th percentile) below, mean = thick line, outliers = circles, whiskers = 90th percentile, above, and 10th percentile, below.

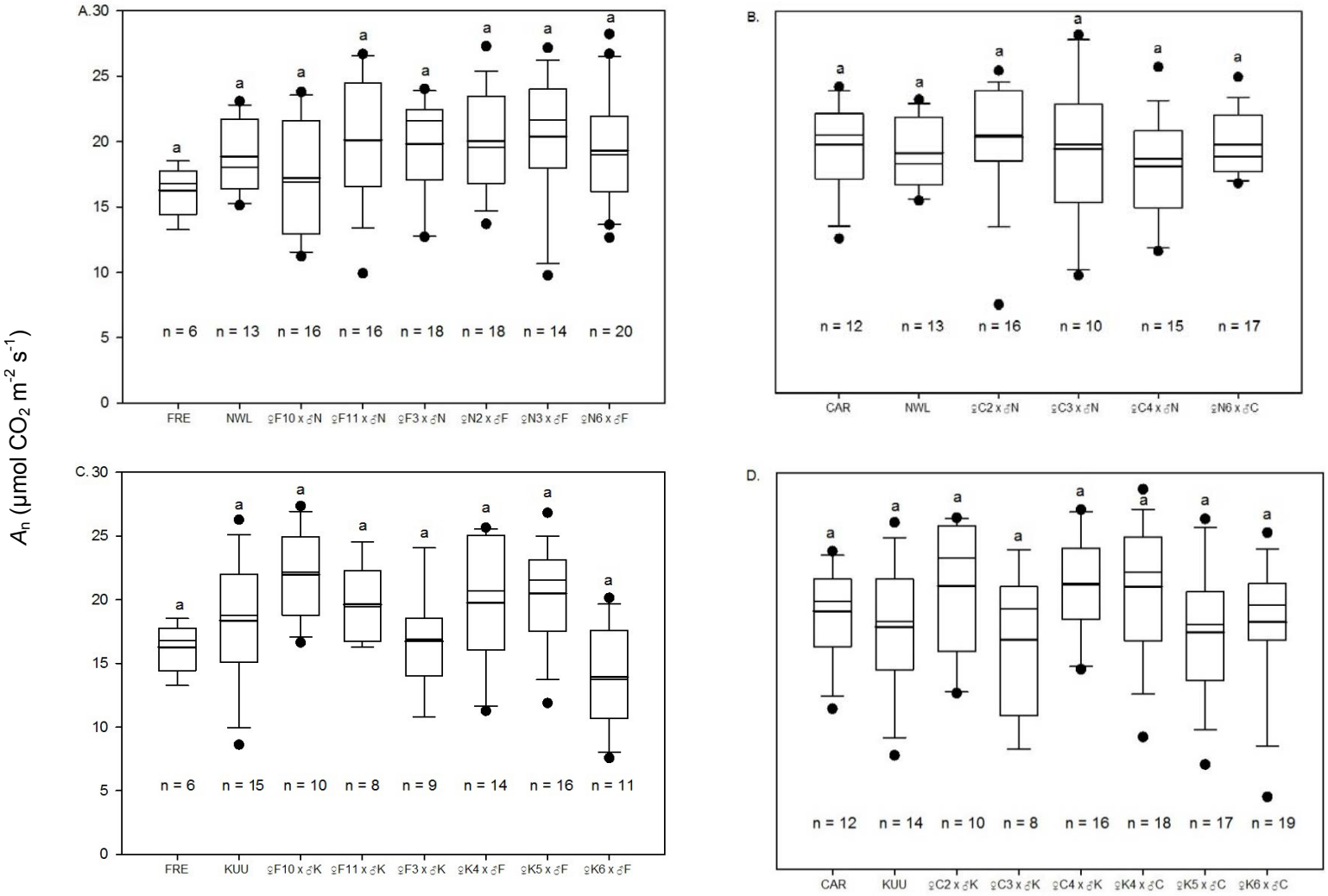

Figure 2.9 Box plots representing the photosynthetic rates (A_n) of the pseudo-parents and the north × south (N×S) families. Median = thin line, quartile (75th percentile) above, 2nd quartile (50th percentile) below mean = thick line, outliers = circles, whiskers = 90th percentile, above, and 10th percentile, below.

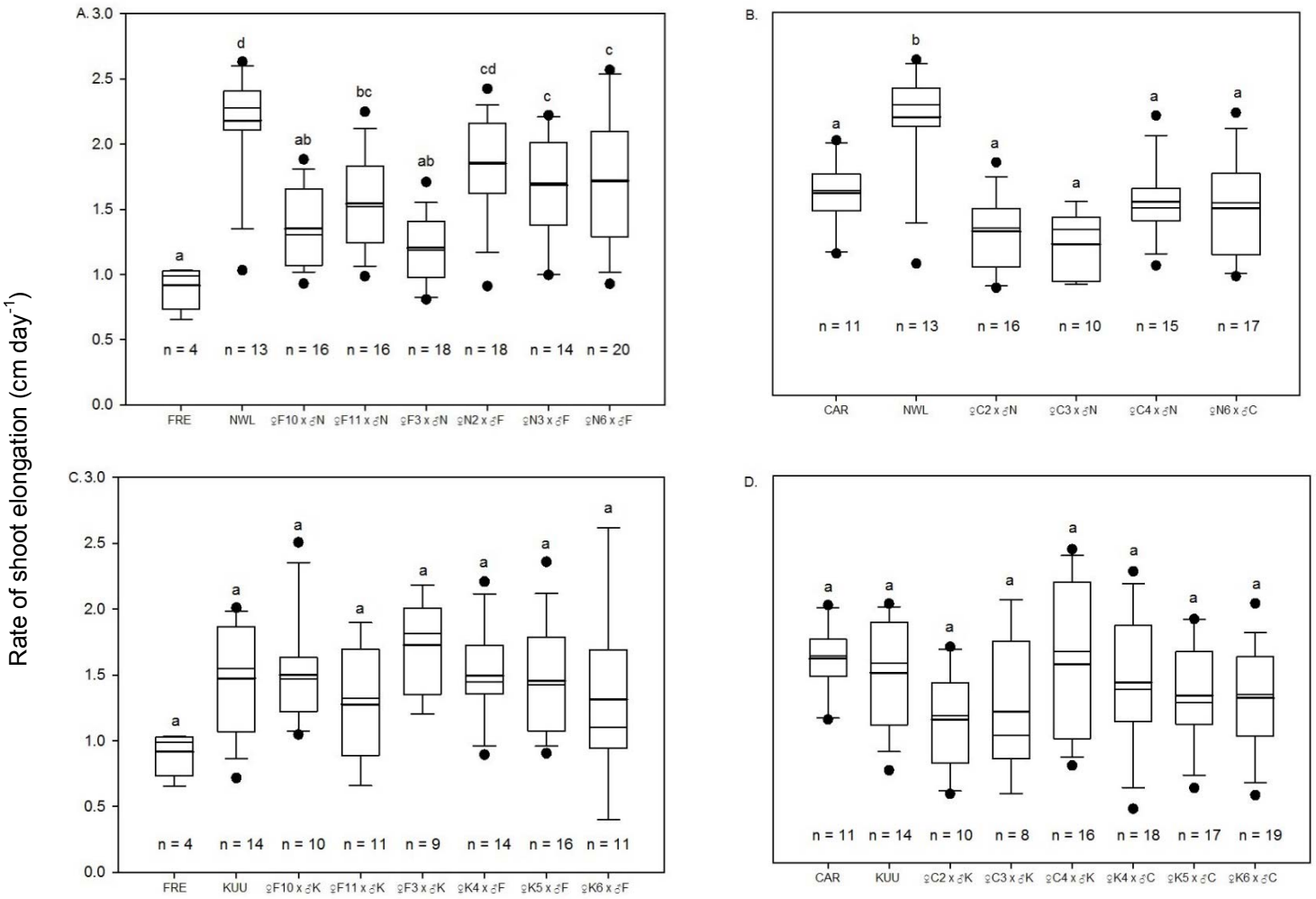

Figure 2.10 Box plots representing the rate of shoot elongation (RSE) of the pseudo-parents and the north × south (N×S) families. Median = thin line; quartile (75th percentile) above, 2nd quartile (50th percentile) below, mean = thick line, outliers = circles, whiskers = 90th percentile, above, and 10th percentile, below.

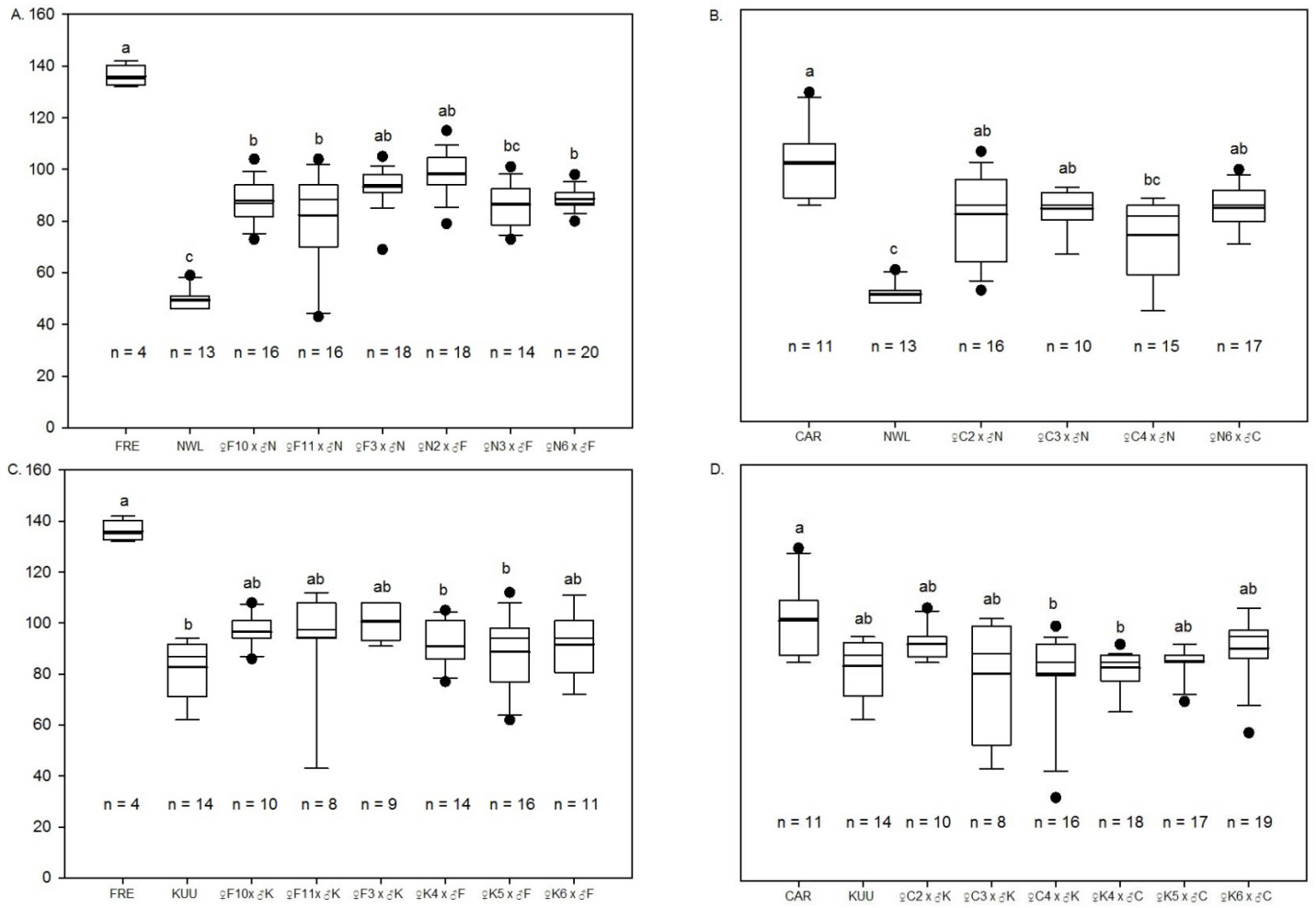

Figure 2.11 Box plots representing the number of days to bud set (DBS) of the pseudo-parents and the north × south (N×S) families. Median = thin line; quartile (75^{th} percentile) above, 2^{nd} quartile (50^{th} percentile) below, mean = thick line, outliers = circles, whiskers = 90^{th} percentile, above, 10^{th} percentile, below.

Table 2.1 The statistically significant (t-stat (RSE) or q-stat (DBS), and *P* value) differences between the N × S cross families and their pseudo-parents.

Rate of shoot elongation (Figure 2.9. A, B)		
Family	**Pseudo-parent**	
	FRE	**NWL**
♀F10 × ♂N	$t_{(7)} = 5.937$, $P < 0.001$	n.s.
♀F11 × ♂N	$t_{(7)} = 4.564$, $P < 0.001$	$t_{(7)} = 3.010$, $P = 0.048$
♀F3 × ♂N	$t_{(7)} = 7.183$, $P < 0.001$	n.s
♀N2 × ♂F	n.s.	$t_{(7)} = 5.144$, $P < 0.001$
♀N3 × ♂F	$t_{(7)} = 3.380$, $P = 0.017$	$t_{(7)} = 3.605$, $P = 0.009$
♀N6 × ♂F	$t_{(7)} = 3.300$, $P = 0.021$	$t_{(7)} = 3.855$, $P = 0.004$
	CAR	**NWL**
♀C2 × ♂N	n.s.	$t_{(5)} = 7.303$, $P < 0.001$
♀C3 × ♂N	n.s.	$t_{(5)} = 7.092$, $P < 0.001$
♀C4 × ♂N	n.s.	$t_{(5)} = 5.405$, $P < 0.001$
♀N6 × ♂C	n.s.	$t_{(5)} = 5.487$, $P < 0.001$
Days to bud set (Figure 2.10 A, B, C, D)		
	FRE	**NWL**
♀F10 × ♂N	$q_{(7)} = 3.220$, $P < 0.05$	$q_{(7)} = 3.546$, $P < 0.05$
♀F11 × ♂N	$q_{(7)} = 3.240$, $P < 0.05$	$q_{(7)} = 3.515$, $P < 0.05$
♀F3 × ♂N	n.s.	$q_{(7)} = 5.324$, $P < 0.05$
♀N2 × ♂F	n.s.	$q_{(7)} = 6.339$, $P < 0.05$
♀N3 × ♂F	$q_{(7)} = 3.373$, $P < 0.05$	n.s.
♀N6 × ♂F	$q_{(7)} = 3.327$, $P < 0.05$	$q_{(7)} = 3.385$, $P < 0.05$
	CAR	**NWL**
♀C2 × ♂N	$q_{(5)} = 4.116$, $P < 0.05$	n.s.
♀C3 × ♂N	$q_{(5)} = 3.631$, $P < 0.05$	n.s.
♀C4 × ♂N	n.s.	$q_{(5)} = 3.662$, $P < 0.05$
♀N6 × ♂C	$q_{(5)} = 3.893$, $P < 0.05$	n.s.
	FRE	**KUU**
♀F10 × ♂K	n.s.	n.s.
♀F11 × ♂K	n.s.	n.s.
♀F3 × ♂K	n.s.	n.s.
♀K4 × ♂F	$q_{(7)} = 3.336$, $P < 0.05$	n.s.
♀K5 × ♂F	$q_{(7)} = 3.281$, $P < 0.05$	n.s.
♀K6 × ♂F	n.s.	n.s.
	CAR	**KUU**
♀C2 × ♂K	n.s.	n.s.
♀C3 × ♂K	n.s.	n.s.
♀C4 × ♂K	$q_{(7)} = 3.192$, $P < 0.05$	n.s.
♀K4 × ♂C	$q_{(7)} = 3.636$, $P < 0.05$	n.s.
♀K5 × ♂C	n.s.	n.s.
♀K6 × ♂C	n.s.	n.s.

CHAPTER 3. Internal mesophyll conductance and water-use efficiency functionally linked to leaf mass area in intra-specific hybrids of *Populus balsamifera* L.

3.1 Introduction

Leaf mass area (LMA) is a measure of the leaf dry-mass per unit of leaf area. Variation in LMA may be due to variation in leaf thickness, leaf mass density, or both (Witkowski and Lamont 1991). A global trend of high LMA in species with long leaf longevity has been reported (Wright et al. 2004). These species likely allocate more resources to building structural components that may provide resistance against abiotic and biotic stress, while species with shorter leaf longevity likely allocate resources to rapid growth (Muir et al. 2014).

Intra-specific variation in LMA has also been reported in geographically widespread tree species (e.g., Laforest-Lapointe et al. 2014; Fajardo and Piper 2011). In *Populus balsamifera* L., high LMA, photosynthetic carbon assimilation rates (A_n), leaf nitrogen content and internal mesophyll conductance (g_m) were all found to be positively correlated with latitude of origin (Soolanayakanahally et al. 2009). The authors partially attributed the high A_n of the northern populations of *P. balsamifera* to high g_m (Soolanayakanahally et al. 2009). However, the increased path length to diffusion of CO_2 that would be expected from thicker leaves is contrary to the high g_m observed in these northern populations. Additionally and/or alternatively, leaves with high LMA could be a result of greater tissue density, which may account for the positive correlation observed between LMA and g_m. Higher cell density, and a larger volume of mesophyll cells and intercellular air spaces accounted for the higher LMA in evergreen species, as compared to deciduous, reported in a study of 26 woody species (Villar et al. 2013). In a study

conducted by Hanba et al. (1999), leaves with large LMA also had thicker mesophyll, larger surface area of mesophyll cells exposed to intercellular air spaces per unit leaf area (S_{mes}/S), and a smaller volume ratio of intercellular spaces relative to the whole mesophyll, known as mesophyll porosity. Internal mesophyll conductance was found to be positively related to S_{mes}/S and negatively related to mesophyll porosity, suggesting that the liquid phase of the diffusion of CO_2 more than the gaseous phase may be responsible for determining g_m (Hanba et al. 1999).

In addition to g_m, Soolanayakanahally et al. (2009) also reported a positive correlation between intrinsic water-use efficiency (WUE_i, μmol CO_2 $mmol^{-1}$ H_2O) and latitude of origin. Differences in the balance between photosynthetic rates and transpiration are responsible for variation in WUE. Greater WUE can be achieved if lower stomatal conductance (g_s, mol H_2O m^{-2} s^{-1}) decreases transpiration rates more than photosynthetic rates, which must be the case if there is no change in internal resistance or carboxylation capacity. Alternatively, an increased intrinsic photosynthetic rate at a given g_s can also increase WUE. An increase in the carboxylation capacity as a result of an increase in the concentration of active Rubisco sites (Whitney et al. 2011) or by an improvement in the enzyme's kinetics could result in greater photosynthetic rates (Galmés et al. 2005). An increase in the diffusion of CO_2 to the site of carboxylation (g_m) may also increase photosynthetic rates, and subsequently WUE, if there is not also a large increase in g_s (Flexas et al. 2013).

Given, the variation in physiological and phenological traits of the F_1s described in Chapter 2, one might also expect a large amount of variation in their LMA. This variation in LMA may provide an opportunity to further elucidate the relationships

between LMA and g_m and other interrelated physiological traits (A_n, WUE, and g_s). In other studies the examination of the intra-specific variation of LMA has been confounded by geographical factors such as latitude of origin (e.g., Soolanayakanahally et al. 2009) and elevation (e.g., Fajardo and Piper 2011). In the study by Soolanayakanahally et al. (2009), the measurements of internal mesophyll conductance were limited to only a few genotypes from just three northern and three southern populations. Latitudinal trends in LMA and g_m, however, may reflect independent selection and not any causal relationship. In contrast, as the F_1 genotypes resulted from crosses between geographically extreme provenances (particularly the northeast by southwest and northwest by southeast crosses), they have no defined latitude or environment of origin. Any observed co-variation in LMA and g_m in these crosses is more likely attributable to a functional dependence of the latter on the former (the possibility of genetic linkage aside). Additionally, many studies that have examined intra-specific variation in LMA and g_m have been *in situ*, where leaves within a canopy or leaves of differing age, developmental stage or sun and shade leaves have been compared (e.g., Montpied et al. 2009), potentially creating or confounding correlations between these traits. In the present study, all genotypes were grown in the greenhouse under constant conditions, and care was taken to reduce self-shading.

The first objective was to determine the LMA of the pseudo-parents and their F_1 progeny to examine relationships between this trait and A_n, g_s, and WUE. The second objective was to further explore the relationship between the internal conductance and LMA by measuring g_m and related biochemical parameters in a north × south *P. balsamifera* family with high variation in LMA.

3.2 Materials and methods

Two experiments were conducted. The first experiment utilized the full set of pseudo-parents and their progeny as described in Chapter 2. The second experiment was restricted to just a single family.

Experiment 1

The source of the plant material, growing conditions and gas exchange methods for the pseudo-parents and their progeny are described in the Materials and Methods section of Chapter 2. In addition to photosynthetic carbon assimilation rate (A_n, μmol CO_2 m^{-2} s^{-1}), the stomatal conductance (g_s, μmol H_2O m^{-2} s^{-1}), and transpiration rate (E, mmol H_2O m^{-2} s^{-1}) were used for analyses in this chapter. The photosynthetic water-use efficiency (WUE, μmol CO_2 $mmol^{-1}$ H_2O) was calculated using A_n and E for the gas exchange data in Chapter 2 with Equation 3.1:

$$\text{WUE} = A_n \text{ (μmol } CO_2 \text{ } m^{-2} \text{ } s^{-1}) \text{ / } E \text{ (mmol } H_2O \text{ } m^{-2} \text{ } s^{-1}) \quad \textbf{(3.1)}$$

Following gas exchange measurements, the leaf in which the measurements were conducted was removed from the plant. A single-hole paper puncher, which produces a disc of known area, was used to take three punches randomly from the whole leaf surface, avoiding the mid-vein. The leaf discs were dried in a 60°C oven for 48 hours and weighed. LMA was calculated by dividing the total mass by the total known area of the three leaf discs.

Experiment 2

The family with the greatest variance in LMA, resulting from a cross between two latitudinally disparate parents was selected to estimate internal mesophyll conductance via *A*-C_i curve fitting. The family selected (♀K4×♂C), has a mother from Kuujjuaq, QC and a father from a poly-blend of three genotypes from Carnduff, SK (refer to Chapter 2). In July 2011, three ramets of each of the nineteen genotypes in this family, each with 2 or 3 buds, were rooted in 4L pots with mixture of Sunshine-2 (Sun Gro Horticulture, Vancouver, Canada) growing mix (60%), peat moss (30%) and vermiculite (10%). Trees were grown in a greenhouse at the University of British Columbia, Vancouver with natural light supplemented by fluorescent lamps to provide a photoperiod of 21 hours to prevent bud set from occurring in the northern parents or their offspring. Day and night temperatures in the greenhouse were maintained at 25°C and 20°C respectively. Trees were watered as needed and staked to ensure vertical growth and reduce self-shading. In addition to regular watering, trees were given a solution of 18-18-18 fertilizer (Plant Products Co., ON, Canada) containing 200ppm of nitrogen once a week for the duration of the study. Pots were fully randomized once a week to minimize any positional effects.

When ramets were 5 weeks old, *A*-*C*i curves were constructed using a LI-6400 gas exchange system (LICOR Instruments, Lincoln, NE, USA) equipped with a red-blue LED unit. The leaf chamber temperature was set to 25ºC and the initial reference CO_2 at 400 μL L^{-1}. Over an interval of 10 minutes the PPFD was ramped up to 1000 μmol m^{-2} s^{-1} while maintaining a VPD inside the leaf chamber close to 1.5 kPa throughout the measurements. The reference CO_2 was then changed in the following order: 400, 500, 630, 700, 800, 900, 1050, 1400, 1200, 970, 850, 750, 570, 450, 250, 100, 50, 200, and

370 μL L^{-1}. These points were chosen to minimize the number of readings that would lead to a C_i between 200 and 300 μL L^{-1}, which should be avoided, as there is a transition from the Rubisco-limited state (~200 μL L^{-1}) to the RuBP-regeneration-limited state (> 300 μL L^{-1}). These points were also chosen in order to prevent any temporal drift in the precision of the gas exchange system. To ensure accurate readings, A_n and g_s were allowed to stabilize before a change in the reference CO_2. The curve fitting computer model developed by Sharkey et al. (2007) was used to estimate the maximum carboxylation rate allowed by Rubisco (V_{cmax}), the rate of photosynthetic electron transport (J), triose phosphate utilization (TPU), day respiration (R_d), and internal mesophyll conductance (g_m). Following gas exchange measurements, LMA was determined on three leaf discs from each leaf in the same manner as described for Experiment 1.

Carbon isotope discrimination analysis

Given the number of assumptions, limitations and sources of error associated with each of the current methods of estimating g_m, multiple methods are usually employed as a way of validating results (Pons et al. 2009). There was, however, a lack of access to the equipment necessary for online isotope discrimination methods, which couple gas exchange measurements with tunable diode laser absorption spectroscopy and can easily measure discrimination in real-time without destructive sampling. I therefore assessed the possibility of obtaining a more immediate, but still destructive measure of discrimination, based on the isotopic analysis of extracted foliage. The results were not conclusive but are presented in Appendix B for reference.

Statistics

All statistical analyses were conducted using SigmaPlot version 13.0 (Systat 2014). One-way analysis of variance (ANOVA on Ranks) was used to test for differences between families, as well as pseudo-parents, in A_n, g_s, WUE, and LMA. The Dunn's method (q-statistic) (Dunn 1964) was used to perform pairwise multiple comparisons. A separate ANOVA was performed to test for clonal variation within the ♀K4×♂C family. Pairwise multiple comparisons were performed according to the Holm-Šidák method (t-statistic) (Holm 1977). A best global fit polynomial, quadratic regression analysis was employed to examine the relationship between A_n, g_s, and WUE with LMA of pseudo-parents and their progeny. Linear regression was used to examine the relationship between A_n, g_s, WUE and g_m with LMA for the ♀K4×♂C family. Pearson's correlations were calculated to determine the relationships between the remaining estimated A-C_i curve fitting parameters (V_{cmax}, J, TPU, R_d) and LMA.

3.3 Results

In Experiment 1, a positive curvilinear relationship was observed between A_n and LMA in the pseudo-parents and their progeny ($r = 0.511$, $r^2 = 0.259$, $P < 0.0001$) (Fig 3.1.A). Stomatal conductance was only weakly correlated with LMA in the pseudo-parents and F1s ($r = 0.270$, $r^2 = 0.070$, $P < 0.0001$) (Fig.3.1.B), but carbon assimilation rates and g_s were well correlated ($r = 0.630$, $r^2 = 0.395$, $P < 0.0001$) with each other (not shown). A positive curvilinear relationship between WUE and LMA in the pseudo-parents and their progeny was also observed ($r = 0.530$, $r^2 = 0.277$, $P < 0.0001$) (Fig. 3.1.C).

Large variation in A_n, g_s, LMA and WUE for pseudo-parents and F_1 families were observed (Table 3.1). There were significant family-level differences in A_n ($P = 0.024$), WUE ($P = 0.011$), and LMA ($P < 0.001$). The ♀K6×♂F family had significantly lower photosynthetic rates than three of the other F_1 families (♀F10×♂K, ♀C4×♂K, and ♀K4×♂C). The ♀K6×♂F family also had significantly lower WUE than the ♀K4×♂C family. Additionally, the FRE pseudo-parent had lower LMA than the NWL pseudo-parent and the ♀N6×♂K family.

Significant clonal variation in g_s ($P < 0.001$) and LMA ($P = 0.014$), but not A_n ($P = 0.061$) or WUE ($P = 0.126$), was detected within the ♀K4×♂C family in Experiment 2 (Table 3.2). There were numerous pairwise differences between clones in g_s but for LMA, only one genotype stood out (i.e., ♀K4×♂C-17 had higher LMA than genotypes 2, 8, 9, 10, 11 15, and 20). Consistent with Experiment 1, there was a significant positive relationship between A_n and LMA among the ♀K4×♂C genotypes ($r = 0.733$, $r^2 = 0.511$, $P = 0.0004$) (Fig. 3.2.A). Strong linear relationships in g_s ($r = 0.581$, $r^2 = 0.299$, $P = 0.0091$) (Fig. 3.2.B) and WUE ($r = 0.620$, $r^2 = 0.349$, $P = 0.0046$) (Fig. 3.2.C) with LMA were observed. Given the trends observed in Fig.3.1, curvilinear relationships between A_n, g_s and WUE with LMA might also be expected in Fig. 3.2, but the smaller sample size precludes detection.

Of the fitted A-C_i curve parameters estimated for the ♀K4×♂C genotypes, a significant positive linear relationship was observed between LMA and both V_{cmax} ($r = 0.535$, $P = 0.018$) (Fig. 3.3.A) and g_m ($r = 0.671$, $r^2 = 0.418$, $P = 0.0017$) (Fig.3.4). While

no significant relationships were observed between LMA and J, TPU, and R_d, TPU and LMA were also weakly correlated with each other (r = 0.391, *P* = 0.098) (Fig. 3.3.C).

3.4 Discussion

In nature, there is great variation in LMA, both among (e.g., Read et al. 2014; Villar et al. 2013; Wyka et al. 2012) and within species (e.g., Laforest-Lapointe et al. 2014; Asner et al. 2011; Fajardo and Piper 2011; Pensa et al. 2010). A positive correlation between LMA and leaf longevity is reported in the 'worldwide leaf economic spectrum' by Wright et al. (2004). For example, long-lived evergreen leaves are thicker than shorter-lived deciduous leaves. Much of this inter-specific variation in LMA can be attributed to differences between biomes and prevalent functional groups (i.e., evergreens, deciduous trees, succulents, etc.), but there is also considerable variation in LMA across species within functional groups (Poorter et al. 2009). Within functional groups, high leaf densities were observed in species with high LMA, while the differences in LMA between functional groups were found to be a result of thicker leaves (Poorter et al. 2009). Conversely, intra-specific variation in LMA likely reflects local adaptation, as variation in LMA in geographically widespread species has been reported within species across environmental and geographical gradients. For example, in a study of *Nothofagus pumilio*, a tree species with a wide latitudinal and altitudinal distribution, LMA co-varied with mean temperatures which varied with elevation (Fajardo and Piper 2011).

In *P. balsamifera*, LMA was reported to co-vary with latitude of origin (Soolanayakanahally et al. 2009). High latitude populations had higher LMA than low latitude populations. In Experiment 1, there was a large amount of variation in the LMA

and gas exchange characteristics of the F_1s and their pseudo-parents (Fig. 3.1.A) but few family-level differences (Table 3.1). A high level of variation, particularly within the crosses, was expected. The low LMA of the pseudo-parent from southeastern Canada relative to at least the pseudo-parent from the Northwest Territories and the ♀N6×♂K family is consistent with latitudinal patterns reported by Soolanayakanahally et al. (2009). In Experiment 2, and despite low replication (3 ramets/clone), significant clonal variation (Table 3.2) was found within the ♀K4×♂C family for LMA and g_s, and nearly so for A_n.

In addition to genotypic differences in LMA, there can be developmental (Tosens et al. 2012), seasonal (McKown et al. 2013) and plastic (e.g., sun vs shade leaves, Terashima et al. 2006) variation in LMA. Variation in LMA was also observed between experiments within this study. The LMA for the ♀K4×♂C ramets grown for the *A*-C_i curve fitting (5.9 to 10.7 mg cm^{-2}) was greater than when they were grown alongside the other F1s and their pseudo-parents (2.3-7.9 mg cm^{-2}) (cf. Fig. 3.2, Tables 3.1 and 3.2). Although the growing conditions (light regime, temperature, etc.) between the greenhouses used in the two experiments were kept as similar as possible, differences in LMA for the same genotypes likely reflect plasticity to growing conditions.

There was a positive relationship between A_n and LMA across all the F_1s and their pseudo-parents (Fig. 3.1.A). Wright et al. (2004) reported a global trend of decreasing mass and area based measurements of photosynthetic rates (A_{mass} and A_{area}) and mass and area based measurements of leaf nitrogen (N_{mass} and N_{area}) with increasing LMA across species. A similar trend was observed in a study of species within the genus *Banksia*, which have traits that fall at one extreme of the leaf trait spectrum (Hassiotou et al. 2010).

High LMA was associated with more leaf tissue, low N_{mass} and low A_{mass}. However, A_{area} and LMA were not correlated despite the positive relationship with mesophyll volume per area (Hassiotou et al. 2010). The authors attributed the low A_{area} to lower internal conductance due to the greater mesophyll cell wall thickness at high LMA. Contrary to the global trend across species, Niinemets (2015) found LMA to be positively correlated with N_{mass} and A_{mass} within *Quercus ilex* L. Likewise, Soolanayakanahally et al. (2009) reported a positive correlation between A_n and LMA across populations of *P. balsamifera*.

High LMA can result from a thick leaf and/or a leaf with high tissue density (Witkowski and Lamont 1991). Leaf thickness and leaf density are both affected by anatomical leaf traits such as cell size and shape, cell surface area, porosity, etc. (Evans and Poorter 2001; Niinemets 1999). In a study of anatomical leaf characteristics encompassing most of the same ♀K4×♂C genotypes used in this chapter, variation in LMA was largely accounted for by combining variation in leaf thickness and leaf density (i.e., mesophyll cell packing) (Milla-Moreno 2014). There were positive correlations between LMA and cell wall area, the surface area of mesophyll cells in the palisade tissue and the surface area of mesophyll cells exposed to air space (S_{mes}/S). Chloroplast numbers were also correlated with S_{mes}/S (Milla-Moreno 2014). Consequently, the high A_n at high LMA may have been a result of an increase in the number of chloroplasts, or photosynthetic "machinery", per unit leaf area, but could also arise from a higher g_m stemming more directly from the increase in S_{mes}/S.

In addition to the positive relationship between A_n and LMA, a positive relationship between WUE and LMA was also observed here (Fig 3.1.C). Water-use

efficiency has been positively correlated with LMA in a number of studies. For example, under variable water and light availability Aranda et al. (2007) found a positive relationship between $\delta^{13}C$ and LMA in *Quercus suber* L., indicating greater WUE at high LMA. In a study of the intra-specific variation in LMA of six woody species, greater internal air volume in leaves, which was reflected in a larger LMA, was positively correlated with water-use efficiency (Mediavilla et al. 2001). The authors suggested that this increase in WUE was likely a result of greater diffusion of CO_2 to the site of carboxylation. A positive correlation between LMA and WUE was also reported in *P. balsamifera* (Soolanayakanahally et al. 2009).

The curvilinear relationship between A_n and LMA, and WUE and LMA, as demonstrated by the global best fit regression (Fig. 3.1), suggests that the maximum photosynthetic rate is reached at an optimal LMA. Beyond this point, increased leaf thickness may limit photosynthesis due to an increase in the path length for the diffusion of CO_2, which reduces g_m. Alternatively, as leaf density increases with LMA, the closely touching cells resulting from the more densely packed tissue could lead to an overlapping of cell walls, ultimately reducing g_m. However, without more genotypes with high LMA (Fig. 3.1), it is difficult to be sure that A_n doesn't simply level off.

The g_s was strongly correlated with A_n ($r = 0.6295$, $r^2 = 0.3953$, $P < 0.0001$), which is as expected, but was only weakly correlated with LMA ($r = 0.2626$, $P < 0.0001$) (Fig. 3.1.B). This suggests that g_m, and not g_s, underlies the relationship between A_n and WUE with LMA. To investigate further, g_m was estimated using A-C_i curve fitting methods. For logistical reasons not all genotypes could be measured, therefore g_m was

estimated for the F1 family with the greatest variation among individuals in LMA; namely, ♀K4×♂C

As was observed in the F1s and their pseudo-parents, the A_n, g_s, and WUE were positively correlated with LMA in the ♀K4×♂C family. However, the increase in g_s with LMA was much lower for the ♀K4×♂C family than for the F_1s and pseudo-parents (cf. Fig.3.1.B, Fig.3.2.B). The relatively small increase in g_s with LMA compared to A_n suggests the greater photosynthetic rates drive the increase in WUE with LMA. The positive correlation between V_{cmax} (the maximum carboxylation rate of Rubisco) and LMA suggests that an increase in photosynthetic rates could be partially attributable to an increase in carboxylation capacity. However, the increase in V_{cmax} was not reflected in an increase in J, TPU and R_d, which might normally be expected, as these estimated biochemical parameters are often correlated with each other.

Correlations between the estimated biochemical parameters and LMA have been reported in the literature. For example, in a study examining seasonal gradients in photosynthetic capacity and internal conductance in the canopy of *Fagus sylvatica* L., V_{cmax}, J_{max} and g_m were all correlated with LMA, which in turn was strongly correlated with local irradiance in the canopy (Montpied et al. 2009). Although V_{cmax}, J_{max} and g_m were not themselves correlated with irradiance, the data suggested a plastic response of LMA for acclimation to the local environment which results in an adjustment of the biochemistry related to photosynthetic capacity (Montpied et al. 2009).

Despite the weak correlations of V_{cmax} and TPU with LMA in the present study (Fig. 3.3), there was a strong positive correlation between g_m and LMA (Fig. 3.4). Although, g_s

and g_m were both positively correlated with LMA in the ♀K4×♂C genotypes, the much greater increase in g_m compared to g_s suggests that g_m played the greater role in determining the photosynthetic rate. In such a scenario, as stomatal conductance becomes more limiting, CO_2 concentrations in the mesophyll space would be drawn down (not shown) and WUE must increase (Fig 3.2.C).

3.5 Conclusion

In this study I have taken advantage of large clonal variation in LMA within a single N×S family to explore the relationship between g_m and overall leaf anatomy in *P. balsamifera* under common, steady-state conditions. It's important to note, however, that internal mesophyll conductance can change rapidly and independently from leaf anatomy in response to changing environmental conditions, such as changes in light and water availability (Griffiths and Helliker 2013; Tazoe et al. 2011; Evans et al. 2009). Rapid changes in g_m may be caused, for example, by aquaporins mediating the diffusion of CO_2 through membranes (Perez-Martin et al. 2014) or changes in chloroplast positioning (Tholen et al. 2008). Nonetheless, the present work shows that g_m and WUE are directly correlated with LMA and may be functionally linked. Leaf anatomy likely determines an upper limit for g_m. In facilitating CO_2 diffusion for carbon assimilation, the clear advantage of an increase in g_m, over an increase in g_s, is that it does not promote further water loss.

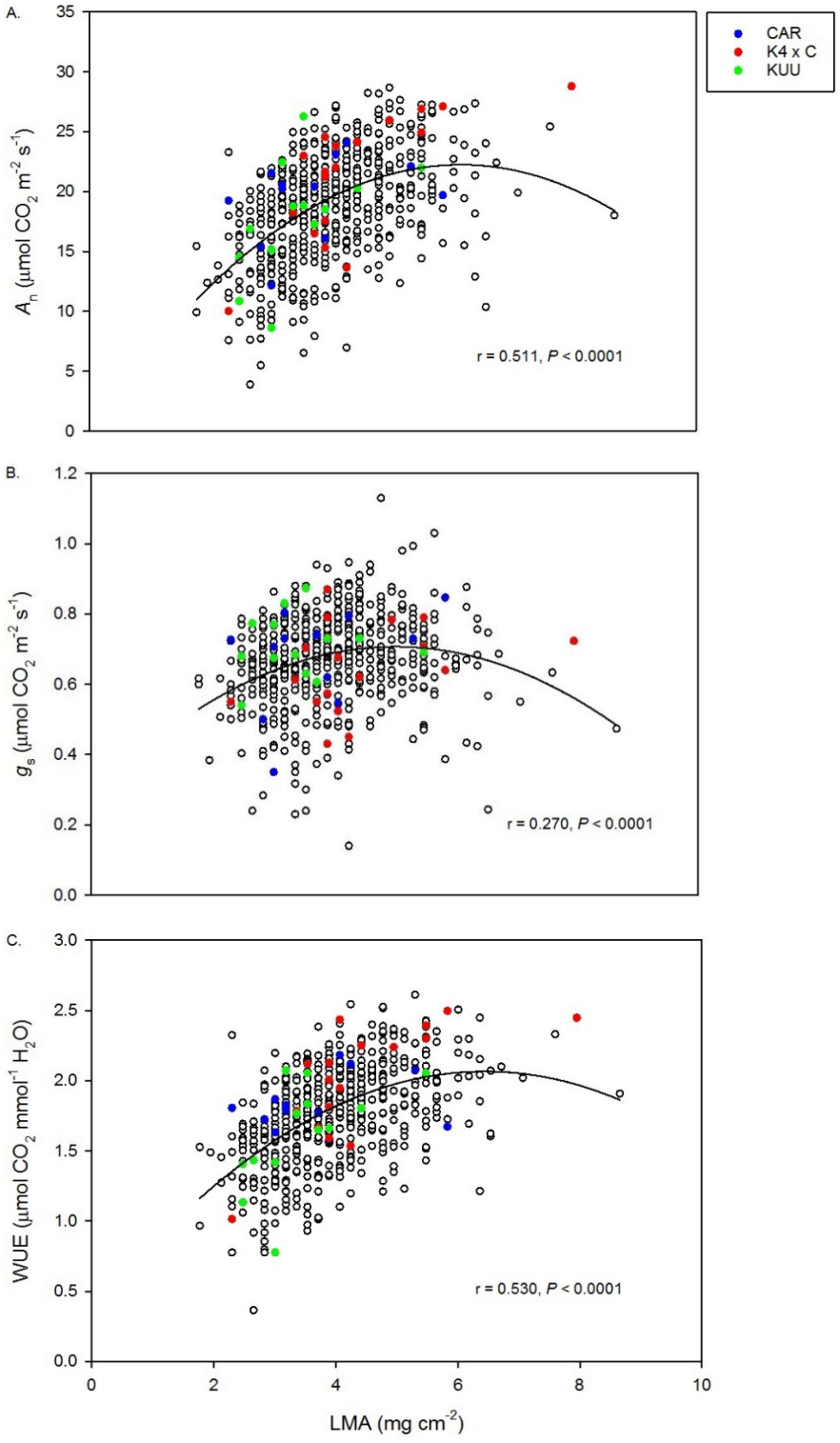

Figure 3.1 The relationship of photosynthetic carbon assimilation rate (A_n) stomatal conductance (g_s), and water-use efficiency (WUE) with leaf-mass area (LMA) of the F_1s and their pseudo-parents. Coloured dots represent the genotypes from the ♀K4×♂C family and its pseudo-parents (KUU and CAR).

Table 3.1 Means and standard deviation (±) of A_n, g_s, WUE, and LMA of the F_1 families and their pseudo-parents. Bold = family (♀K4×♂C) and pseudo-parents selected for Experiment 2; n = sample size; significant differences between families denoted by different superscript letters ($P < 0.05$).

Parent/Family	n	A_n	g_s	WUE	LMA
CAR	**9**	**19.55 ± 3.43^{ab}**	**0.67 ± 0.14**	**1.84 ± 0.19^{ab}**	**3.71 ±1.04^{ab}**
FRE	6	16.28 ± 1.94^{ab}	0.62 ± 0.09	1.58 ± 0.17^{ab}	2.80 ± 0.44^{b}
KUU	**13**	**17.72 ± 4.75^{ab}**	**0.71 ± 0.09**	**1.62 ± 0.38^{ab}**	**3.44 ± 0.83^{ab}**
NWL	13	18.88 ± 2.80^{ab}	0.65 ± 0.10	1.82 ± 0.22^{ab}	5.00 ± 1.52^{a}
♀C2 × ♂C	15	19.04 ± 4.99^{ab}	0.67 ± 0.13	1.78 ± 0.37^{ab}	3.98 ± 0.77^{ab}
♀C3 × ♂C	11	19.27 ± 4.30^{ab}	0.58 ± 0.11	1.93 ± 0.37^{ab}	4.27 ± 0.74^{ab}
♀C4 × ♂C	18	18.98 ± 3.83^{ab}	0.65 ± 0.13	1.81 ± 0.34^{ab}	4.45 ± 1.04^{ab}
♀C2 × ♂F	12	17.37 ± 4.88^{ab}	0.68 ± 0.19	1.68 ± 0.30^{ab}	3.90 ± 0.77^{ab}
♀C3 × ♂F	11	17.27 ± 4.44^{ab}	0.58 ± 0.06	1.69 ± 0.42^{ab}	3.50 ± 0.96^{ab}
♀C4 × ♂F	13	17.87 ± 4.84^{ab}	0.69 ± 0.07	1.67 ± 0.45^{ab}	3.93 ± 0.96^{ab}
♀C2 × ♂K	10	21.46 ± 5.26^{ab}	0.70 ± 0.10	1.97 ± 0.42^{ab}	4.29 ± 0.89^{ab}
♀C3 × ♂K	6	11.21 ± 6.25^{ab}	0.33 ± 0.29	1.10 ± 0.82^{ab}	2.37 ± 1.54^{ab}
♀C4 × ♂K	15	21.79 ± 3.77^{a}	0.75 ± 0.13	1.95 ± 0.23^{ab}	4.15 ± 0.84^{ab}
♀C2 × ♂N	15	19.89 ± 4.54^{ab}	0.68 ± 0.17	1.89 ± 0.25^{ab}	4.11 ± 0.89^{ab}
♀C3 × ♂N	10	19.23 ± 5.44^{ab}	0.64 ± 0.14	1.84 ± 0.44^{ab}	4.08 ± 0.75^{ab}
♀C4 × ♂N	14	17.63 ± 3.98^{ab}	0.60 ± 0.18	1.75 ± 0.25^{ab}	4.74 ± 1.05^{ab}
♀F3 × ♂C	16	17.44 ± 5.10^{ab}	0.66 ± 0.13	1.65 ± 0.40^{ab}	4.19 ± 1.10^{ab}
♀F10 × ♂C	18	17.92 ± 5.32^{ab}	0.65 ± 0.10	1.68 ± 0.42^{ab}	3.41 ± 0.76^{ab}
♀F11 × ♂C	16	18.61 ± 4.58^{ab}	0.68 ± 0.15	1.73 ± 0.32^{ab}	3.72 ± 1.06^{ab}
♀F3 × ♂F	11	16.76 ± 5.91^{ab}	0.68 ± 0.19	1.57 ± 0.39^{ab}	3.71 ± 0.85^{ab}
♀F10 × ♂F	3	19.79 ± 6.43^{ab}	0.81 ± 0.11	1.69 ± 0.53^{ab}	3.81 ± 2.01^{ab}
♀F11 × ♂F	7	18.13 ± 3.42^{ab}	0.69 ± 0.12	1.72 ± 0.26^{ab}	3.61 ± 1.06^{ab}
♀F3 × ♂K	8	16.78 ± 4.08^{ab}	0.67 ± 0.09	1.57 ± 0.39^{ab}	4.26 ± 1.00^{ab}
♀F10 × ♂K	12	21.95 ± 3.38^{a}	0.74 ± 0.07	1.94 ± 0.30^{ab}	3.99 ± 1.00^{ab}
♀F11 × ♂K	8	19.63 ± 2.96^{ab}	0.74 ± 0.09	1.78 ± 0.25^{ab}	3.82 ± 1.06^{ab}
♀F3 × ♂N	18	19.83 ± 3.90^{ab}	0.66 ± 0.09	1.87 ± 0.32^{ab}	4.11 ± 0.80^{ab}
♀F11 × ♂N	16	20.11 ± 4.65^{ab}	0.74 ± 0.15	1.80 ± 0.32^{ab}	3.92 ± 1.07^{ab}

Table 3.1 Continued

Parent/Family	n	A_n	g_s	WUE	LMA
♀F10 × ♂N	16	17.22 ± 4.58^{ab}	0.68 ± 0.10	1.64 ± 0.40^{ab}	3.91 ± 0.87^{ab}
♀K4 × ♂C	**18**	**21.40 ± 5.16^{a}**	**0.65 ± 0.12**	**2.01 ± 0.39^{a}**	**4.38 ± 1.23^{ab}**
♀K5 × ♂C	17	17.95 ± 5.00^{ab}	0.71 ± 0.15	1.62 ± 0.33^{ab}	3.90 ± 0.94^{ab}
♀K6 × ♂C	19	18.74 ± 4.84^{ab}	0.67 ± 0.14	1.76 ± 0.38^{ab}	3.56 ± 0.85^{ab}
♀K4 × ♂F	13	19.55 ± 5.21^{ab}	0.66 ± 0.15	1.86 ± 0.37^{ab}	3.86 ± 0.85^{ab}
♀K5 × ♂F	16	20.50 ± 3.83^{ab}	0.70 ± 0.11	1.88 ± 0.30^{ab}	3.88 ± 0.62^{ab}
♀K6 × ♂F	11	13.95 ± 3.81^{b}	0.57 ± 0.09	1.41 ± 0.34^{b}	3.31 ± 0.81^{ab}
♀K5 × ♂K	12	19.45 ± 4.10^{ab}	0.74 ± 0.08	1.74 ± 0.35^{ab}	3.77 ± 0.86^{ab}
♀K6 × ♂K	10	18.64 ± 3.77^{ab}	0.70 ± 0.09	1.72 ± 0.38^{ab}	3.75 ± 0.93^{ab}
♀K4 × ♂N	14	20.44 ± 4.80^{ab}	0.65 ± 0.14	1.92 ± 0.30^{ab}	4.03 ± 0.89^{ab}
♀K5 ×♂N	15	17.12 ± 4.63^{ab}	0.62 ± 0.14	1.69 ± 0.40^{ab}	3.78 ± 1.01^{ab}
♀K6 × ♂N	13	18.64 ± 3.77^{ab}	0.69 ± 0.07	1.74 ± 0.33^{ab}	3.71 ± 1.12^{ab}
♀N6 × ♂C	17	19.55 ± 2.48^{ab}	0.65 ± 0.09	1.87 ± 0.19^{ab}	4.30 ± 0.84^{ab}
♀N2 × ♂F	16	19.61 ± 3.49^{ab}	0.74 ± 0.13	1.78 ± 0.26^{ab}	4.19 ± 0.67^{ab}
♀N3 × ♂F	14	20.37 ± 5.06^{ab}	0.75 ± 0.10	1.78 ± 0.39^{ab}	3.76 ± 0.81^{ab}
♀N6 × ♂F	20	19.30 ± 4.26^{ab}	0.67 ± 0.14	1.79 ± 0.30^{ab}	4.27 ± 1.01^{ab}
♀N6 × ♂K	18	19.68 ± 2.81^{ab}	0.69 ± 0.07	1.83 ± 0.23^{ab}	4.65 ± 0.94^{a}
♀N6 × ♂N	13	19.76 ± 5.09^{ab}	0.60 ± 0.13	1.96 ± 0.43^{ab}	4.73 ± 1.26^{ab}

A_n, net photosynthetic carbon assimilation rate (μmol CO_2 m^{-2} s^{-1}); g_s, stomatal conductance (μmol CO_2 m^{-2} s^{-1}); WUE, water-use efficiency (μmol CO_2 $mmol^{-1}$ H_2O); LMA, leaf-mass area (mg cm^{-2}). CAR, Carnduff; FRE, Fredericton; KUU, Kuujjuaq; NWL, Norman Wells.

Table 3.2 Means and standard deviation (±) of A_n, g_s, WUE, and LMA of the ♀K4×♂C family; n = sample size; significant differences between clones denoted by different superscript letters ($P < 0.05$).

Genotype	N	A_n	g_s	WUE	LMA
♀K4 × ♂C-1	3	23.68 ± 2.23	0.56 ± 0.015^{bd}	2.37 ± 0.32	9.73 ± 3.08^{ab}
♀K4 × ♂C-2	3	18.49 ± 3.39	0.52 ± 0.007^{ac}	1.97 ± 0.28	6.50 ± 1.93^{a}
♀K4 × ♂C-3	3	18.66 ± 1.76	0.58 ± 0.006^{d}	1.85 ± 0.20	7.67 ± 0.96^{ab}
♀K4 × ♂C-4	3	18.59 ± 3.08	0.51 ± 0.015^{ac}	1.96 ± 0.28	7.41 ± 3.08^{ab}
♀K4 × ♂C-5	3	20.41 ± 1.49	0.57 ± 0.010^{b}	1.99 ± 0.34	8.85 ± 1.45^{ab}
♀K4 × ♂C-6	3	20.47 ± 3.57	0.55 ± 0.009^{d}	2.08 ± 0.44	8.72 ± 1.25^{ab}
♀K4 × ♂C-7	3	19.63 ± 0.72	0.59 ± 0.011^{b}	1.97 ± 0.19	7.18 ± 1.10^{ab}
♀K4 × ♂C-8	3	18.06 ± 3.53	0.52 ± 0.005^{c}	1.89 ± 0.28	6.25 ± 1.30^{a}
♀K4 × ♂C-9	3	16.54 ± 1.27	0.49 ± 0.011^{ac}	1.77 ± 0.21	5.99 ± 2.74^{a}
♀K4 × ♂C-10	3	17.33 ± 2.76	0.50 ± 0.004^{ac}	1.87 ± 0.22	5.96 ± 1.72^{a}
♀K4 × ♂C-11	3	21.57 ± 2.13	0.56 ± 0.017^{d}	2.22 ± 0.26	6.60 ± 1.21^{a}
♀K4 × ♂C-12	3	16.69 ± 1.49	0.56 ± 0.011^{bd}	1.68 ± 0.21	8.28 ± 3.29^{ab}
♀K4 × ♂C-13	3	20.88 ± 2.41	0.55 ± 0.006^{d}	2.25 ± 0.31	8.50 ± 1.88^{ab}
♀K4 × ♂C-14	3	19.36 ± 0.95	0.57 ± 0.010^{b}	1.95 ± 0.12	8.34 ± 2.90^{ab}
♀K4 × ♂C-15	3	17.63 ± 2.61	0.54 ± 0.025^{bd}	1.83 ± 0.21	6.79 ± 2.51^{a}
♀K4 × ♂C-17	3	22.99 ± 1.32	0.57 ± 0.009^{b}	2.32 ± 0.25	10.71 ± 0.76^{b}
♀K4 × ♂C-18	3	18.75 ± 3.07	0.57 ± 0.010^{b}	1.90 ± 0.21	7.84 ± 1.39^{ab}
♀K4 × ♂C-19	3	21.36 ± 1.32	0.54 ± 0.011^{c}	2.15 ± 0.23	8.12 ± 2.17^{ab}
♀K4 × ♂C-20	3	17.98 ± 2.06	0.56 ± 0.009^{bd}	1.82 ± 0.20	6.56 ± 2.37^{a}

A_n, net photosynthetic carbon assimilation rate (μmol CO_2 m^{-2} s^{-1}); g_s, stomatal conductance (μmol CO_2 m^{-2} s^{-1}); WUE, water-use efficiency (μmol CO_2 $mmol^{-1}$ H_2O); LMA, leaf-mass area (mg cm^{-2}).

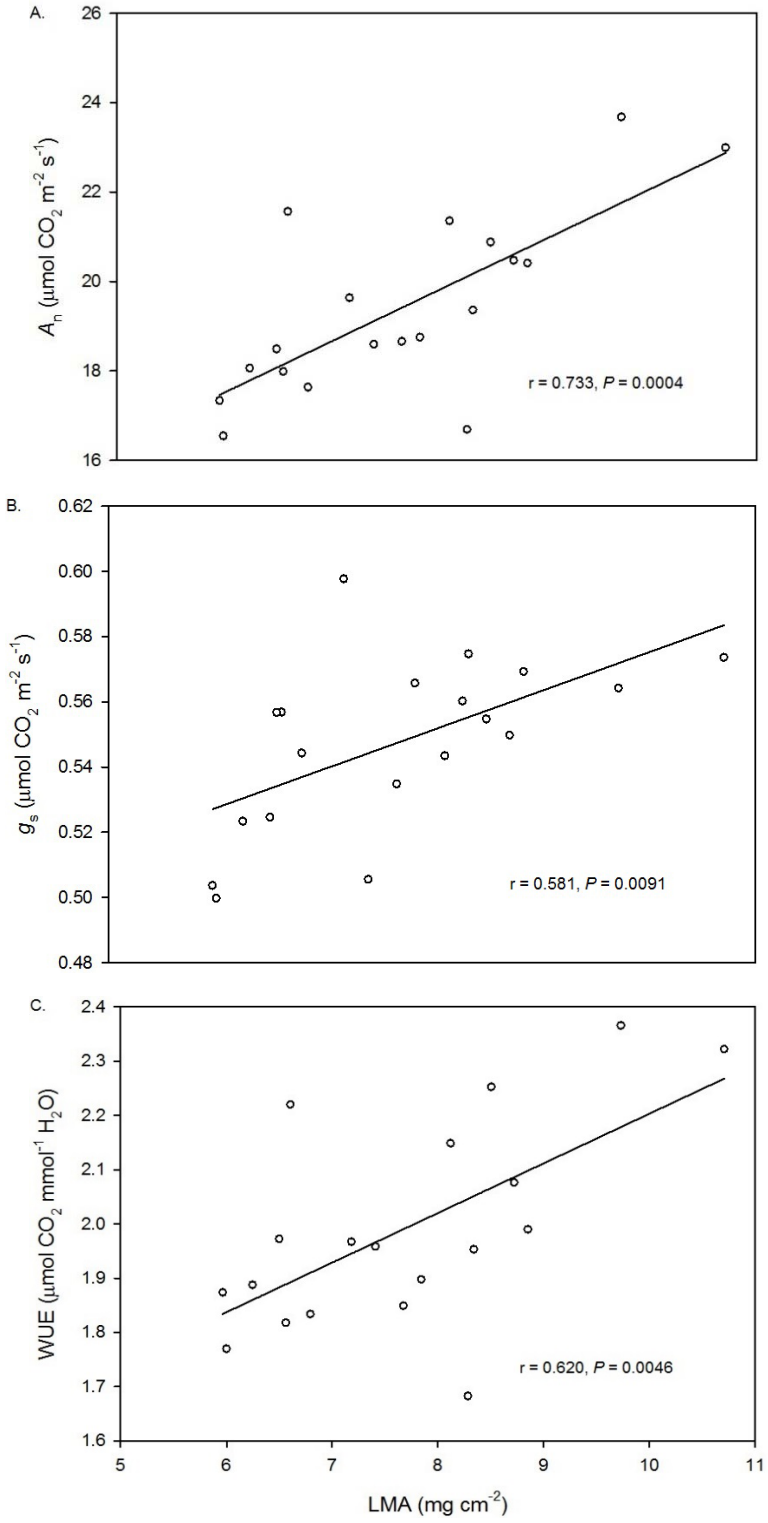

Figure 3.2 The relationship of mean (n = 3) photosynthetic carbon assimilation rate (A_n) stomatal conductance (g_s), and water-use efficiency (WUE) with leaf-mass area (LMA) of the ♀K4×♂C family. Values for A_n and g_s reported are from the A-C_i gas exchange data at near ambient CO_2 (400 µL L^{-1}).

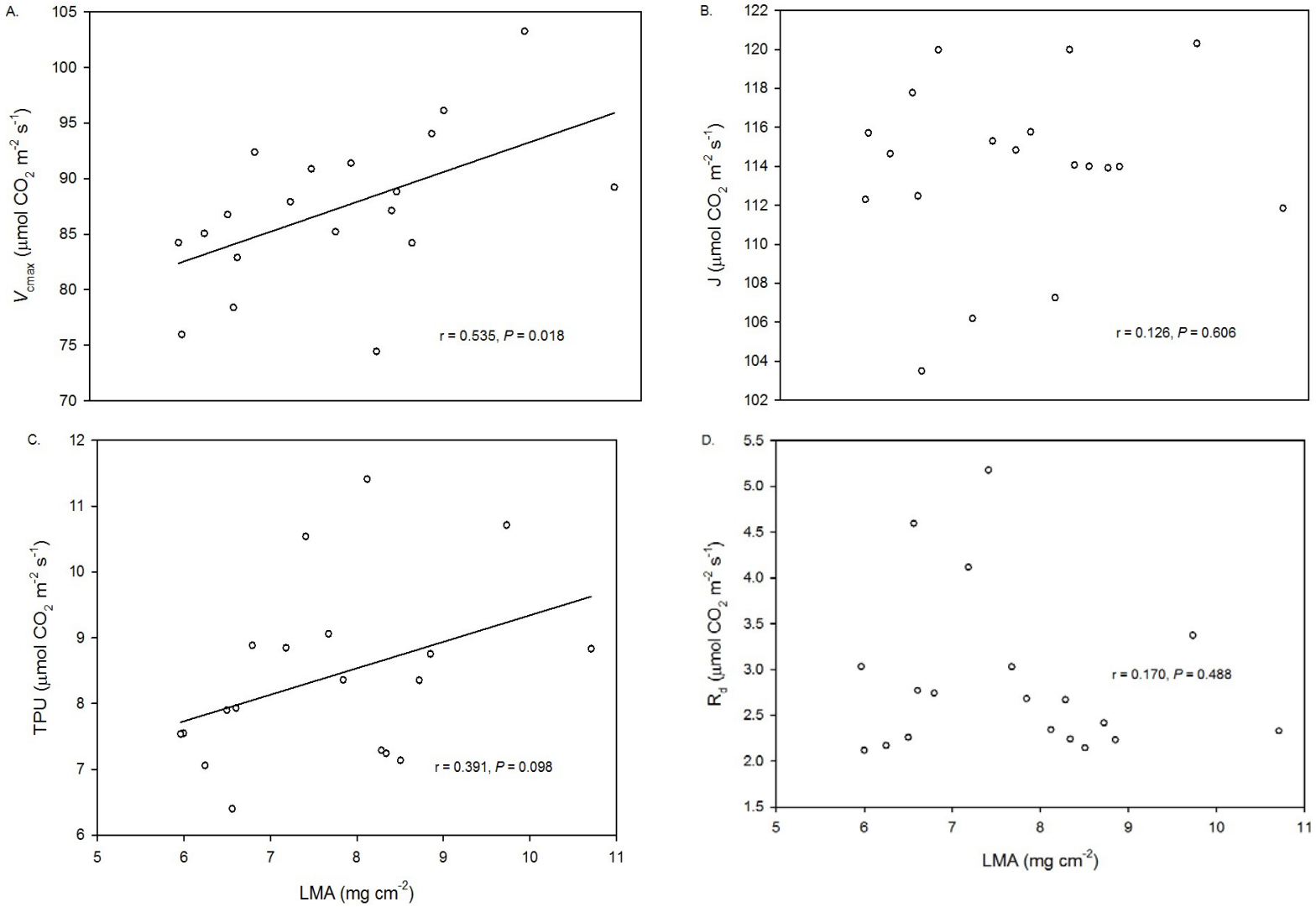

Figure 3.3 The relationship of the mean (n = 3) maximum carboxylation rate of Rubisco (V_{cmax}), the rate of photosynthetic electron transport (J), triose phosphate utilization (TPU), and day respiration (R_d) with leaf-mass area (LMA) of the ♀K4×♂C family as estimate through A-C_i curve fitting.

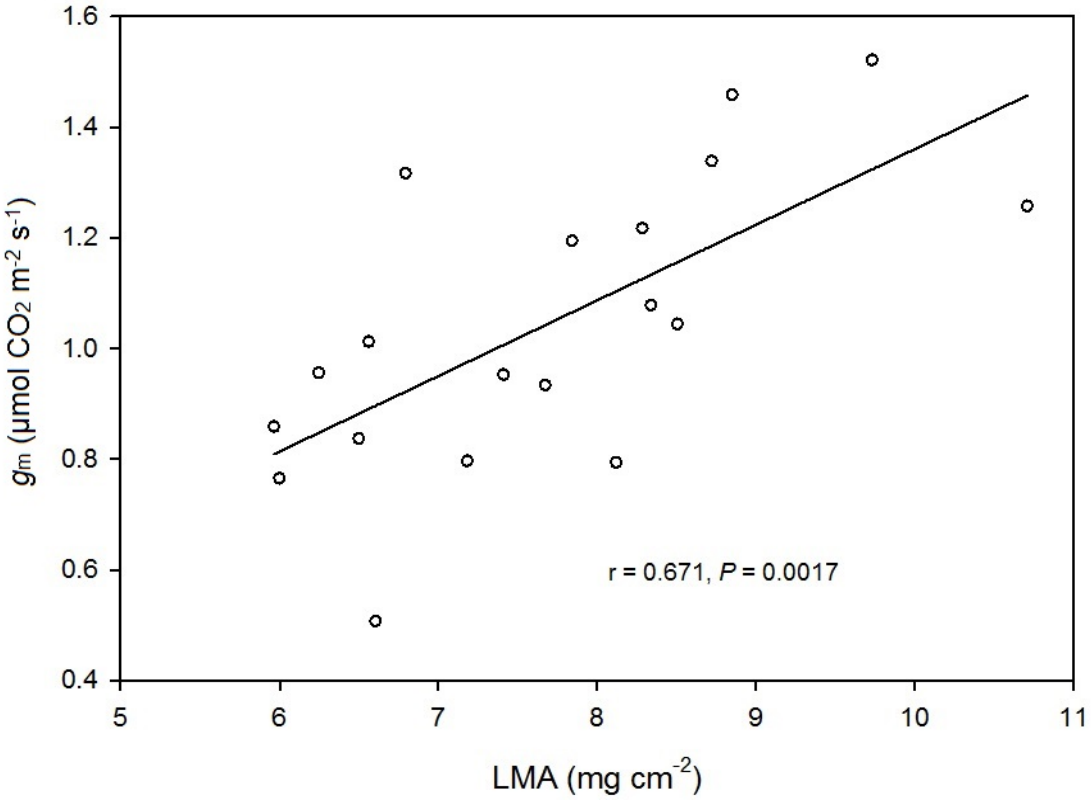

Figure 3.4 The relationship between mean internal mesophyll conductance (g_m) and leaf-mass area (LMA) in the ♀K4×♂C family as estimated from *A*-C_i curve fitting.

Chapter 4. Thesis conclusions

4.1 Introduction

An apparent trade-off between photosynthetic carbon assimilation and growth cessation in *P. balsamifera* exists in nature. The first objective of conducting reciprocal crosses between geographically distant populations of *P. balsamifera* was to attempt to uncouple intrinsic growth potential and phenology and thereby produce fast growing genotypes. Additionally, given the large amount of trait variation expected for progeny of crosses between geographically distant populations, the second objective of the study was to further elucidate the relationships between LMA, A_n, WUE, g_s, and g_m in the F_1 crosses.

4.2 Intrinsic growth potential and phenology can be uncoupled

While the rates of shoot extension and DBS were correlated across all F_1s, in the progeny resulting from crosses between northern and southern parents, they were found to be uncorrelated, which suggests that indeed, intrinsic growth potential and phenology were uncoupled in these genotypes. Overall, the variation in A_n and RSE across all F_1s appeared to be greater than in the pseudo-parents, while there appeared to be much lower variation in DBS in pseudo-parents and F_1s, likely due to the complexity of genes related to phenology. Within this variation a number of genotypes with a combination of high A_n, RSE, and DBS were identified as possible candidates for further exploration.

4.3 WUE and g_m may be functionally linked with LMA

Although a rapid response of WUE and g_m to a changing environment, independent of leaf anatomy has been reported in the literature, in the study described in Chapter 2, WUE and g_m were directly correlated with LMA. By facilitating the diffusion of CO_2, high g_m appeared to confer greater photosynthetic rates in leaves with high LMA. Although g_s was also positively correlated with LMA in the ♀K4×♂C family, the high WUE in leaves with high LMA suggests that the contribution of g_m to photosynthetic rates exceeds any increase in water loss due to greater g_s. However, the potentially curvilinear relationships of g_m and WUE with LMA suggest that there may be an upper optimal limit to LMA, likely as a result of limitations due to leaf anatomy.

4.4 Limitations of the present study

In Chapter 2, the original parental genotypes could not be propagated and therefore genotypes from the same latitudes of origin as the parents (pseudo-parents) had to be used as a representation of the original parents. While the poly-blends of male parents would have precluded the ability to compare F_1 families directly with their fathers, not having the original parental material also meant that the A_n, RSE and DBS of the F_1 families could not be directly compared to their mothers. Without being able to directly compare parents with their progeny, it is very difficult to know whether or not the mean A_n, RSE and DBS of some of the F_1 families might be greater than either or both of their parents (heterosis). While there appeared to be some F_1 families which had outliers for some traits, without an F_2 generation it is difficult to know whether transgressive segregation may produce extreme phenotypes outside of the parental range. Additionally, the unequal sample sizes across all pseudo-parents and F_1s meant that the

ANOVAs used to compare the F_1s with each other and their pseudo-parents did not always show significance, even when the box plots appeared to show differences in traits (for example, see Fig. 2.5.B).

A number of assumptions and a great deal of error are associated with all of the current methods for estimating g_m and other related biochemical and physiological parameters reported in the literature. In addition to error associated with the IRGA, such as gasket leaks, many potential sources of error exist when using the curve fitting computer model developed by Sharkey et al. (2007). One of the biggest sources of error is in the determination of which data points are limited by Rubisco, RuBP regeneration or TPU, which is done using broad criteria that relies on the assumption of validity of the Farquhar et al. (1980) model of C_3 photosynthesis for all species. Also, given the time consuming nature of A-C_i curve fitting, only three replicates of each genotype in one F_1 family could be examined. Without the examination of more genotypes it is difficult to determine whether the correlations of g_m and WUE with LMA hold across all F_1 families.

4.5 Future studies

The common garden of F_1s and their pseudo-parents, which was established and described in Chapter 2, continues to grow and could be used for complimentary field studies. An evaluation of the F_1s in the field would determine whether the combination of high A_n, RSE, and DBS, observed in many of the F_1s, persists in the field. In addition to the rate of shoot elongation and total height, other measures of growth, such as diameter at breast height could be used to further assess intrinsic growth potential. If these measures of growth are correlated with photosynthetic rates in the field, in the same way that A_n and RSE were correlated across F_1s when grown in the greenhouse, candidate F_1s

should accomplish greater growth than their pseudo-parents in the field. Additionally, with all of the genetic material available in the outdoor common garden, an F_2 generation could be produced, focusing primarily on candidate genotypes. Similar analyses could be performed on F_2 families to examine any evidence of transgressive segregation.

Given the error associated with A-C_i curve fitting methods in estimating g_m and other related biochemical parameters, additional methods of estimation should be undertaken to validate the findings from this study. Currently, chlorophyll fluorescence and a unique method of 'online' carbon isotope discrimination are being used to estimate g_m in the ♀K4×♂C family by a colleague (Mina Momayyezi, PhD candidate). As LMA may be a function of either leaf thickness or leaf density and with the strong correlations of physiological traits with LMA observed in this study, detailed exploration of leaf anatomy is also needed. Anatomical leaf characteristics related to g_m and LMA have been examined in the ♀K4×♂C family by Milla-Moreno (2014). While LMA was correlated to a number of anatomical characters, studies of leaf anatomy and g_m have not been conducted on the same material at the time, and it cannot yet be concluded that g_m varies as a specific function of any particular aspect of leaf ultrastructure in the ♀K4×♂C family. Comparisons across studies are likely to be compromised by the plasticity of LMA to growing conditions (as observed, for example, between experiments in the present study). Therefore, future work should focus on simultaneous measurements of g_m and leaf anatomy, and perhaps with genotypes from other F_1 families.

Literature Cited

Aitken SN, Yeaman S, Holliday JA, Wang T, Curtis-McLane S. (2008). Adaptation, migration or extirpation: climate change outcomes for tree populations. *Evolutionary Applications* **1**: 95-111.

Alberto, FJ, Aitken SN, Alía R, González-Martínez SC, Hänninen H, Kremer A, Lefèvre F, Lenormand T, Yeaman S, Whetten R, Savolainen O. (2013). Potential for evolutionary responses to climate change- evidence from tree populations. *Global Change Biology* **19**: 1645-1661.

Aranda I, Pardos M, Puertolas J, Jimenez MD, Pardos JA. (2007). Water-use efficiency in cork oak (*Quercus suber*) is modified by the interaction of water and light availabilities. *Tree Physiology* **27**: 671-677.

Arnold ML, Cornman RS, Martin NH. (2008). Hybridization, hybrid fitness and the evolution of adaptions. *Plant Biosystems* **142**: 166-171.

Arntz AM, Delph LF. (2001). Pattern and process: evidence of the evolution of photosynthetic traits in natural populations. *Oecologia* **127**: 455-467.

Asner GP, Martin RE, Tupayachi R, Emerson R, Martinez P, Sinca F, Powell GVN, Wright SJ, Lugo AE. (2011). Taxonomy and remote sensing of leaf mass per area (LMA) in humid tropical forests. *Ecological Applications* **21**: 85-98.

Benowicz A, El-Kassaby YA, Guy RD, Ying CC. (2000a). Sitka alder (*Alnus sinuata* Rydb.) genetic diversity in germination, frost hardiness and growth attributes. *Silvae Genetica* **49**: 206-212.

Benowicz A, Guy RD and El-Kassaby YA (2000b). Geographic pattern of genetic variation in photosynthetic capacity and growth in two hardwood species from British Columbia. *Oecologia* **123**: 168-174.

Benowicz A, Guy RD, Carlson MR, El-Kassaby YA (2001). Genetic variation among paper birch (*Betula papyrifera* Marsh.) populations in germination, frost hardiness, gas exchange and growth. *Silvae Genetica* **50**: 7-13.

Böhlenius H, Huang T, Charbonnel-Campaa L, Brunner AM, Jansson S, Strauss SH, Nilsson O. (2006). CO/FT regulatory module controls timing of flowering and seasonal growth cessation in trees. *Science* **312**: 1040-1043.

Bradshaw WE, Zani PA, Holzapfel CM. (2004). Adaptation to temperate climates. *Evolution* **58**: 1748-1762.

Burke JM, Voss TJ, Arnold ML (1998). Genetic interactions and natural selection in Louisiana iris hybrids. *Evolution* **52**: 1304-1310.

Burke JM and Arnold ML. (2001). Genetics and the fitness of hybrids. *Annual Review of Genetics* **35**: 31-52

Ceulemans R, Scarascia Mugnozza GT, Wiard BM, Braatne JH, Hinkley TM, Stettler RF. (1992). Production physiology and morphology of *Populus* species and their

hybrids grown under short rotation. I. Clonal comparisons of 4-year growth and phenology. *Canadian Journal of Forest Research* **22**: 1937-1948.

Chen ZJ. (2013). Genomic and epigenetic insights into the molecular bases of heterosis. *Nature Reviews* **14**: 471-482.

Chmura DJ. (2006). Phenology differs among Norway spruce populations in relation to local variation in altitude of maternal stands in the Beskidy Mountains. *New Forests* **32**: 21-31.

Cockerham CC, Zeng ZB. (1996). Design III with marker loci. *Genetics* **143**: 1437-1456.

Cooke JEK, Eriksson ME, Junttila O. (2012). The dynamic nature of bud dormancy in trees: environmental control and molecular mechanisms. *Plant, Cell and Environment* **35**: 1707-1728.

Davenport CB. (1908). Degeneration, albinism and inbreeding. *Science* **28**: 455.

DeVincente MC, Tanksley SD. (1993). QTL analysis of transgressive segregation in an interspecific tomato cross. *Genetics* **134**: 585-596.

Dunn, OJ. (1964). Multiple comparisons using rank sums. *Technometrics* **6**: 241-252.

East EM. (1908). Inbreeding in corn. *Reports of the Connecticut Agricultural Experiments Station for 1907*: 419-428.

Evans JR, von Caemmerer S. (1996). Carbon dioxide diffusion inside leaves. *Plant Physiology* **110**: 339–346.

Evans JR, Poorter H. (2001). Photosynthetic acclimation of plants to growth irradiance: the relative importance of specific leaf area and nitrogen partitioning in maximizing carbon gain. *Plant, Cell and Environment* **24**: 755-767.

Evans JR, Sharkey TD, Berry JA, Farquhar GD. (1986) Carbon isotope discrimination measured with gas exchange to investigate CO_2 diffusion in leaves of higher plants. *Australian Journal of Plant Physiology* **13**: 281- 292.

Evans JR, Kaldenhoff R, Genty B, Terashima I. (2009). Resistances along the CO_2 diffusion pathway inside leaves. *Journal of Experimental Botany* **60**: 2235–2248.

Excoffier L, Ray N. (2008). Surfing during population expansions promotes genetic revolutions and structuration. *Trends in Ecology & Evolution* **23**: 347–351.

Fajardo A, Piper FI. (2011). Intraspecific trait variation and covariation in a widespread tree species (*Nothofagus pumilio*) in southern Chile. *New Phytologist* **189**: 259-271.

Farquhar GD, von Caemmerer S, Berry JA. (1980) A biochemical model of photosynthetic CO_2 assimilation in leaves of C3 species. *Planta* **149**: 78–90.

Farquhar GD, Ehleringer JR, Hubick KT. (1989). Carbon isotope discrimination and photosynthesis. *Annual Review of Plant Physiology and Plant Molecular Biology* **40**: 503-537.

Field C, Merino J and Mooney HA. (1983). Compromises between water-use efficiency and nitrogen-use efficiency in five species of California evergreens. *Oecologia* **60**: 384-389.

Fischer RA. (1918). The correlation between relatives on the supposition of Medelian inheritance

Flexas J, Niinemets U, Gallé A, Barbour MM, Centritto M, Diaz-Espejo A, Douthe C, Galmés J, Ribas-Carbo M, Rodriguez PL, Rosselló F, Soolanayakanahally R, Tomas M, Wright IJ, Farquhar GD, Medrano H. (2013). Diffusional conductances to CO_2 as a target for increasing photosynthesis and photosynthetic water-use efficiency. *Photosynthesis Research* **117**: 45-59.

Fracheboud Y, Luquez V, Björkén L, Sjödin A, Tuominen H, Jansson S. (2009). The control of autumn senescence in European aspens (*Populus tremula*). *Plant Physiology* **149**: 1982-1991.

Galmés J, Flexas J, Keys AJ, Cifre J, Mitchell RAC, Madgwick PJ, Haslam RP, Medrano H, Parry MAJ. (2005). Rubisco specificity factor tends to be larger in plant species from drier habitats and in species with persistent leaves. *Plant, Cell and Environment* **28**: 571–579.

Gornall JL and Guy RD (2007). Geographic variation in ecophysiological traits of black cottonwood (*Populus trichocarpa*). *Canadian Journal of Botany* **85**: 1202-1213.

Griffiths H, Helliker BR. (2013). Mesophyll conductance: internal insights of leaf carbon exchange. *Plant, Cell and Environment* **36**: 733-735.

Guy RD, Reid DM, Krouse HR. (1986). Factors affecting $^{13}C/^{12}C$ ratios of inland halophytes. I. controlled studies on growth and isotopic composition of *Puccinellia nuttalliana* (Schultes) Hitch. *Canadian Journal of Botany* **64**: 2693–2699.

Hanba YT, Miyazawa S-I, Terashima I. (1999). The influence of leaf thickness on the CO_2 transfer conductance and leaf stable carbon isotope ratio for some evergreen tree species in Japanese warm-temperate forests. *Functional Ecology* **13**: 632-639.

Hassiotou F, Renton M, Ludwig M, Evans JR, Veneklaas EJ. (2010). Photosynthesis at an extreme end of the leaf trait spectrum: how does it relate to high leaf dry mass per area and associated structural parameters? *Journal of Experimental Botany*, **61**: 3015-3028.

Harfouche A, Bahrman N, Baradat P, Guyon JP, Petit RJ, Kremer A. (2000). Provenance hybridization in a diallel mating scheme of maritime pine (*Pinus pinaster*). II. Heterosis. *Canadian Journal of Forest Research* **30**: 10-16.

Heide OM. (1974). Growth and dormancy in Norway spruce (Picea abies). I. Interaction of photoperiod and temperature. *Physiologia Plantarum* **30**: 1-12.

Hewitt GM. (2000). The genetic legacy of the Quaternary ice ages. *Nature* 405: 907–913.

Hofer T, Ray N, Wegmann D, Excoffier L. (2009). Large allele frequency differences between human continental groups are more likely to have occurred by drift during range expansions than by selection. *Annals of Human Genetics*: **73**: 95–108.

Holliday JA, Ritland K, Aitken SN. (2010). Widespread, ecologically relevant genetic markers developed from association mapping of climate-related traits in Sitka spruce (*Picea sitchensis*). *New Phytologist* **188**: 501-514.

Holm S. (1979). A simple sequentially rejective multiple test procedure. *Scandinavian Journal of Statistics* **6**: 65–70.

Howe GT, Hackett WP, Furnier GR, Klevorn RE. (1995). Photoperiodic responses of a northern and southern ecotype of black cottonwood. *Physiologia Plantarum* **93**: 695-708.

Howe GT, Aitken SN, Neale DB, Jermstad KD, Wheeler NC, Chen THH (2003). From genotype to phenotype: unraveling the complexities of cold adaptation in forest trees. *Canadian Journal of Botany* **81**: 1247-1266.

Hurme P, Repo T, Savolainen O, Pääkkönen T. (1997). Climatic adaptation of bud set and frost hardiness in Scots pine (*Pinus sylvestris*). *Canadian Journal of Forest Research* **27**: 716-723.

Ingvarsson PK, Garcia MV, Hall D, Luquez V, Jansson S. (2006). Clinal variation in *phyB2*, a candidate gene for day-length-induced growth cessation and bud set, across a latitudinal gradient in European aspen (*Populus tremula*). *Genetics* **172**: 1845-1853.

Iwasaki T, Aoki K, Seo A, Murakami N. (2012). Comparative phylogeography of four component species of deciduous broad-leaved forests in Japan based on chloroplast DNA variation. *Journal of Plant Research* **125**: 207-221.

Johnston AJ, Dieters MJ, Dungey HS, Wallace HM. (2003). Intraspecific hybridization in *Pinus caribaea* var. *hondurensis* I. Performance for growth and form traits. *Euphytica* **129**: 147-157.

Junttila O. (1980). Effect of photoperiod and temperature on apical growth cessation in two ecotypes of *Salix* and *Betula*. *Physiologa Plantarum* **48**: 347-352.

Junttila O and Skaret G (1990). Growth and survival of seedlings of various *Picea* species under northern climatic conditions. *Scandinavian Journal of Forest Research* **5**: 69-81.

Keller SR, Olson MS, Silim SN, Schroeder W, Tiffin P. (2010). Genomic diversity, population structure, and migration following rapid range expansion in the balsam Poplar, *Populus balsamifera*. *Molecular Ecology* **19**: 1212-1226.

Keller SR, Soolanayakanahally RY, Guy RD, Silim S, Olson MS, Tiffin P. (2011). Climate-driven local adaptation of ecophysiology and phenology in balsam poplar, *Populus balsamifera* L. (Salicaceae). *American Journal of Botany* **98**: 99-108.

Laforest-Lapointe I, Martinez-Vilalta J, Retana J. (2014). Intraspecific variability in functional traits matters: case study of Scots pine. *Oecologia* **175**: 1337-1348.

Lauteri M, Scartazza A, Guido MC, Brugnoli E. (1997). Genetic variation in photosynthetic capacity, carbon isotope discrimination and mesophyll conductance in provenance of *Castanea sativa* adapted to different environments. *Functional Ecology* **11**: 675-683.

Marino BD, McElroy MB. 1991. Isotopic composition of atmospheric CO_2 inferred from carbon in C4 plant cellulose. *Nature* **349**: 127–131.

McKown AD, Guy RD, Azam MS, Drewes EC, Quamme LK. (2012). Seasonality and phenology alter functional leaf traits. *Oecologia* **172**: 653-665.

McKown AD, Klápště J, Guy RD, Geraldes A, Porth I, Hannemann J, Friedmann M, Muchero W, Tuskan GA, Ehlting J, Cronk QCB, El-Kassaby YA, Mansfield SD, Douglas CJ. (2014a). Genome-wide association implicates numerous genes underlying ecological trait variation in natural populations of *Populus trichocarpa*. *New Phytologist* **203**: 535-553.

McKown AD, Guy RD, Quamme L, Klápště J, La Mantia J, Constabel CP, El-Kassaby YA, Hamelin RD, Zifkin M, Azam MS. (2014b). Association genetics, geography and ecophysiology link stomatal patterning in *Populus trichocarpa* with carbon gain and disease resistance trade-offs. *Molecular Ecology* **23**: 5771-5790.

Mediavilla S, Escudero A, Heilmeier H. (2001). Internal leaf anatomy and photosynthetic resource-use efficiency: interspecific and intraspecific comparisons. *Tree Physiology* **21**: 251-259.

Milla-Moreno E. (2014). Structural properties related to mesophyll conductance and underlying variation in leaf mass area of balsam poplar (*Populus balsamifera* L.). University of British Columbia, Vancouver, Canada.

Montpied P, Granier A, Dreyer E. (2009). Seasonal time-course of gradients of photosynthetic capacity and mesophyll conductance to CO2 across a beech (Fagus sylvatica L.) canopy. *Journal of Experimental Botany* **60**: 2407-2418.

Morgenstern EK. (1978). Range-wide genetic variation of black spruce. *Canadian Journal of Forest Research* **8**: 463-473.

Muir CD, Hangarter RP, Moyle LC, Davis PA. (2014). Morphological and anatomical determinants of mesophyll conductance in wild relatives of tomato (*Solanum* sect. *Lycopersicon*, sect. *Lycopersicoides*; Solanaceae). *Plant, Cell and Environment* **37**: 1415-1426.

Ni Z, Kim E-D, Ha M, Lackey E, Liu J, Zhang Y, Sun Q, Chen ZJ. (2009). Altered circadian rhythms regulate growth vigour in hybrids and allopolyploids. *Nature* **457**: 327-333.

Nienstaedt H and Olson JS. (1961). Effects of photoperiod and source on seedling growth of eastern hemlock. *Forest Science* **7**: 81-96.

Niinemets U. (1999) Research review. Components of leaf dry mass per area – thickness and density – alter leaf photosynthetic capacity in reverse directions in woody plants. *New Phytologist* **144**: 35-47.

Niinemets U. (2015). Is there a species spectrum within the world-wide leaf economics spectrum? Major variations in leaf functional traits in the Mediterranean sclerophyll Quercus ilex. *New Phytologist* **205**: 79-96.

Olson MS, Levsen N, Soolanayakanahally RY, Guy RD, Schroeder WR, Keller SR, Tiffin P. (2010). The adaptive potential of *Populus balsamifera* L. to phenology requirements in a warmer global climate. *Molecular Ecology* **22**: 1214-1230.

Parkhurst DF, Mott KA. (1990). Intercellular diffusion limits to CO_2 uptake in leaves. *Plant Physiology* **94**: 1024-1032.

Pensa M, Karu H, Luud A, Kund K. (2010). Within-species correlations in leaf traits of three boreal plant species along a latitudinal gradient. *Plant Ecology* **208**: 155-166.

Perez-Martin A, Michelazzo C, Torres-Ruiz JM, Flexas J, Fernández, Sebastiani L, Diaz-Espejo A. (2014). Regulation of photosynthesis and stomatal and mesophyll conductance under water stress and recovery in olive trees: correlation with gene expression of carbonic anhydrase and aquaporins. *Journal of Experimental Botany* **65**: 3143-3156.

Petit JR, Aguinagalde I, de Beaulieu J-L, Brewer S, Cheddadi R, Ennos R, Fineschi S,Grivet D, Lascoux M, Mohanty A, Müller-Starck G, Demesure-Musch B, Palmé A, Martín JP, Rendell S, Vendramin GG. (2003). Glacial refugia: hotspots but not melting pots of genetic diversity. *Science* **300**: 1563-1565.

Pointeau VM, Guy RD. (2014). Comparative resource-use efficiencies and growth of *Populus trichocarpa* and *Populus balsamifera* under glasshouse conditions. *Botany* **92**: 443-451.

Pons TJ, Flexas J, von Caemmerer S, Evans JR, Genty B, Ribas-Carbo M, Brugnoli E.(2009). Estimating mesophyll conductance to CO_2: methodology, potential errors, and recommendations. *Journal of Experimental Botany* **60**: 2214-2234.

Poorter H, de Jong R. (1999). A comparison of specific leaf area, chemical composition and leaf construction costs of field plants from 15 habitats differing in productivity. *New Phytologist* **143**: 163-176.

Poorter H, Niinemets U, Poorter L, Wright IJ, Villar R. (2009). Causes and consequences of variation in leaf mass per area (LMA): a meta-analysis. *New Phytologist* **182**: 565-588.

Rancourt GT, Éthier G, Pepin S. (2015). Greater efficiency of water use in poplar clones having a delayed response of mesophyll conductance to drought. *Tree Phyisiology* **35**: 172-184.

Read QD, Moorhead LC, Swenson NG, Bailey JK, Sanders NJ. (2014). Convergent effects of elevation on functional leaf traits within and among species. *Functional Ecology* **28**: 37-45.

Reich PB, Ellsworth DS, Walters MB et al. (1999). Generality of leaf trait relationships: a test across six biomes. *Ecology* **80**: 1955-1969.

Rieseberg LH, Sinervo B, Linder CR, Ungerer MC, Arias DM. (1996). Role of gene interactions in hybrid speciation: evidence from ancient and experimental hybrids. *Science* **272**: 741-745.

Savolainen O, Pyhajarvi T. (2007). Genomic diversity in forest trees. *Current Opinion in Plant Biology* **10**: 162–167.

Saxe H, Cannell MGR, Johnson O, Ryan MG, Vourlitis G. (2001). Tree and forest functioning in response to global warming. *New Phytologist* **149**: 369-400.Scafaro AP, von Caemmerer S, Evans JR, Atwell BJ. (2011). Temperature response of mesophyll conductance in cultivated and wild *Oryza* species with contrasting mesophyll cell wall thickness. *Plant, Cell and Environment* **34**: 1999–2008.

Schmidtling RC, Nelson CD. (1996). Interprovenance crosses in loblolly pine using selected parents. *Forest Genetics* **3**: 53-66.

Schull GH. (1908). The composition of a field of maize. *Reports of the American Breeders Association*: 296-301.

Sharkey TD, Bernacci CJ, Farquhar GD, Singsaas EL. (2007). Fitting photosynthetic carbon dioxide response curves for C3 leaves. *Plant, Cell and Environment* **30**: 1035-1040.

Sinha SK, Khanna S. (1975). Physiological, biochemical, and genetic basis of heterosis. *Advanced Agronomy* **27**: 123-174.

Slatkin M, Lande R. (1994). Segregation variance after hybridization of isolated populations. *Genetics Research (Cambridge)***64**: 51-56.

Soolanayakanahally RY, Guy RD, Silim SN, Drewes EC, Schroeder WR. (2009). Enhanced assimilation rate and water use efficiency with latitude through increased photosynthetic capacity and internal conductance in balsam poplar (*Populus balsamifera* L.). *Plant, Cell and Environment* **32**: 1821–1832.

Soolanayakanahally RY, Guy RD, Silim SN, Song M. (2013). Timing of photoperiodic competency causes phenological mismatch in balsam poplar (*Populus balsamifera* L.). *Plant Cell Environment* **36**: 116-127.

Stuber GW, Lincoln SE, Wolff DW, Helentjaris T, Lander ES. (1992). Identification of genetic factors contributing to heterosis in a hybrid from two elite maize inbred lines using genetic markers. *Genetics* **132**: 823-839.

Taberlet P, Fumagalli L, Wust-Saucy A-G, Cosson J-F. (1998). Comparative phylogeography and postglacial colonization routes in Europe. *Molecular Ecology* **7**: 453-464.

Tazoe Y, Caemmerer S, Estavillo GM, Evans JR. (2011).Using tunable diode laser spectroscopy to measure carbon isotope discrimination and mesophyll conductance to CO_2 diffusion dynamically at different CO_2 concentrations. *Plant, Cell and Environment* **34**: 580-591.

Terashima I, Hanba YT, Tazoe Y, Vyas P, Yano S. (2006). Irradiance and phenotype: comparative eco-development of sun and shade leaves in relation to photosynthetic CO_2 diffusion. *Journal of Experimental Botany* **57**: 343–54.

Terashima I, Hanba YT, Tholen D, Niinemets Ü. (2011). Leaf functional anatomy in relation to photosynthesis. *Plant Physiology* **155**: 108–16.

Tholen D, Boom C, Noguchi K, Ueda S, Katase T, Terashima I. (2008). The chloroplast avoidance response decreases internal conductance to CO_2 diffusion in *Arabidopsis thaliana* leaves. *Plant, Cell and Environment* **31**: 1688-1700.

Tosens T, Niinemets Ü, Vislap V, Eichelmann H, Castro Díez P. (2012). Developmental changes in mesophyll diffusion conductance and photosynthetic capacity under different light and water availabilities in *Populus tremula*: How structure constrains function. *Plant, Cell and Environment* **35**: 839–856.

Tuskan GA, Difazio S, Jansson S, Bohlmann J, Grigoriev I, Hellsten U, Putnam N, Ralph S, Rombauts S, Salamov A, Schein J, Sterck L, Aerts A, Bhalerao RR, Bhalerao RP, Blaudez D, Boerjan W, Brun A, Brunner A, Busov V, Campbell M, Carlson J, Chalot M, Chapman J, Chen GL, Cooper D, Coutinho PM, Couturier J, Covert S, Cronk Q, Cunningham R, Davis J, Degroeve S, Déjardin A, Depamphilis C, Detter J, Dirks B, Dubchak I, Duplessis S, Ehlting J, Ellis B, Gendler K, Goodstein D, Gribskov M, Grimwood J, Groover A, Gunter L, Hamberger B, Heinze B, Helariutta Y, Henrissat B, Holligan D, Holt R, Huang W, Islam-Faridi N,Jones S, Jones-Rhoades M, Jorgensen R, Joshi C, Kangasjärvi J, Karlsson J, Kelleher C, Kirkpatrick R, Kirst M, Kohler A, Kalluri U, Larimer F, Leebens-Mack J, Leplé JC, Locascio P, Lou Y, Lucas S, Martin F, Montanini B, Napoli C, Nelson DR, Nelson C, Nieminen K, Nilsson O, Pereda V, Peter G, Philippe R, Pilate G, Poliakov A, Razumovskaya J, Richardson P, Rinaldi C, Ritland K, Rouzé P, Ryaboy D, Schmutz J, Schrader J, Segerman B, Shin H, Siddiqui A, Sterky F, Terry A, Tsai CJ, Uberbacher E, Unneberg P, Vahala J, Wall K, Wessler S, Yang G, Yin T, Douglas C, Marra M, Sandberg G, Van de Peer

Y, Rokhsar D. (2006). The genome of black cottonwood, *Populus trichocarpa* (Torr. & Gray). *Science* **313**: 1596-1604.

Vihera-Aarnio A, Hakkinen R, Junttila O. (2006). Critical night length for bud set and its variation in two photoperiodic ecotypes of Betula pendula. *Tree Physiology* **26**: 1013-1018.

Villar R, Ruiz-Robleto J, Ubera JL, Poorter H. (2013). Exploring variation in leaf mass per area (LMA) from leaf to cell: an anatomical analysis of 26 woody species. *American Journal of Botany* **100**: 1969–1980.

Wang H, McArthur ED, Sanderson SC, Graham JH, Freeman DC. (1997).Natural hybrid zone between two subspecies of big sagebrush (*Artemisia tridentata*: Asteraceae). 4. Reciprocal transplant experiments. *Evolution* **51**: 95-102.

Warren CR, Ethier GJ, Livingston NJ, Grant NJ, Turpin DH, Harrison DL, Black TA. (2003). Transfer conductance in second growth Douglas-fir (*Pseudotsuga menziesii* (Mirb.) Franco) canopies. *Plant, Cell and Environment* **26**: 1215-1227.

Warren CR. (2006). Estimating the internal conductance to CO_2 movement. *Functional Plant Biology* **33**: 431–442.

Warren CR. (2008). Stand aside stomata, another actor deserves centre stage: the forgotten role of the internal conductance to CO_2 transfer. *Journal of Experimental Botany* **59**:1475-1487.

Warren CR and Adams MA. (2006). Internal conductance does not scale with photosynthetic capacity: implications for carbon isotope discrimination and the economics of water and nitrogen use in photosynthesis. *Plant Cell and Environment* **29**: 192-201.

Wuehlisch G. von, Krusche D and Muhs HJ. (1995). Variation in temperature sum requirement for flushing of beech provenances. *Silvae Genetica* **44**: 343-346.

Whitney M, Houtz RL, Alonso H. (2011). Advancing our understanding and capacity to engineer nature's CO_2-sequestering enzyme, Rubisco. *Plant Physiology* **155**: 27-35.

Williams JW, Shuman BN, Webb T, Bartlein PJ, Leduc PL. (2004). Late-quaternary vegetation dynamics in North America: scaling from taxa to biomes. *Ecological Monographs* **74**: 309–334.

Witkowski ETF, Lamont BB. (1991). Leaf specific mass confounds leaf density and thickness. *Oecologia* **88**: 486-493.

Worrall J. (1983). Temperature-bud burst relationships in amabilis and subalpine fir provenance tests replicated at different elevations. *Silvae Genetica* **32**: 203-209.

Wright IJ, Reich PB, Westoby M, Ackerly DD, Baruch Z, Bongers F, Cavender-Bares J, Chapin T, Cornelissen JHC, Diemer M, Flexas J, Garnier E, Groom PK, Gulias J, Hikosaka K, Lamont BB, Lee T, Lee W, Lusk C, Midgley JJ, Navas ML, Niinemets Ü, Oleksyn J, Osada N, Poorter H, Poot P, Prior L, Pyankov VI, Roumet C, Thomas

SC, Tjoelker MG, Veneklaas EJ, Villar R. (2004). The worldwide leaf economics spectrum. *Nature* **428**: 821–827.

Yu SB, Li JX, Xu CG, Gao YJ, Li XH, Zhang Q, Maroof MAS. (1997). Importance of epistasis as the genetic basis of heterosis in an elite rice hybrid. *Protocols of the National Academy of Science USA* **94**: 9226-9231.

Xiao J, Li J, Yuan L, Tanksley SD. (1996). Identification of QTLs affecting traits of agronomic importance in a recombinant inbred population derived from a subspecific rice cross. *Theoretical Applied Genetics* **92**: 230-244.

APPENDIX A. Carbon isotope discrimination analysis as an estimate of internal mesophyll conductance (g_m)

A.1 Introduction

Full expression of potential carbon isotope discrimination (Δ) by Rubisco is dependent on the free and unrestricted diffusion of CO_2 from the atmosphere to the enzyme (Farquhar et al. 1989). The theoretical isotope discrimination expected if there were only stomatal limitations to CO_2 diffusion can be calculated from the measurement of stomatal conductance (i.e., by gas exchange analysis). The difference between the observed discrimination (Δ_{obs}) and the theoretical discrimination (Δ_i) reflects an estimate of the internal mesophyll conductance to CO_2 (Evans et al. 1986, Evans and von Caemmerer 1996). Ideally, the observed/actual discrimination is observed at the same time as gas exchange measurements are performed, so that Δ_{obs} and Δ_i may be compared directly. Isotope discrimination can be measured "on-line" by monitoring the isotopic composition (the $\delta^{13}C$ value) of CO_2 in air entering and leaving the gas exchange cuvette. This approach requires access to a tunable diode laser spectrophotometer. Alternatively, air samples can be collected in flasks and the CO_2 purified cryogenically (and tediously) for analysis on an isotope ratio mass spectrometer. Neither technique was available to me, so I explored the possibility of obtaining a measure of Δ_{obs} based on the isotopic analysis of extracted foliage, in the hope that the soluble aqueous fraction would carry an isotopic signature consistent with the recent photosynthetic activity of the leaf. I hoped that comparison of this value with the $\delta^{13}C$ of source air would provide an estimate of Δ_{obs} encompassing the period over which gas exchange measurements were performed.

A.2 Materials and methods

Plant material

Three of the 41 cross families were selected based on the LMA calculated in Chapter 3. The family with the greatest (♀C4×♂N) and the lowest (♀K6×♂F) mean LMA, and the family with the greatest variance in LMA (♀K4×♂ C) were selected, as individuals with varying leaf thickness and/or density may have observable differences in estimated g_m. For information about the source of the plant material and growing conditions please refer to Chapter 2.

Leaf Tissue

The leaves on which gas exchange measurements were taken in Chapter 2 were immediately packed in vials and quickly frozen in liquid nitrogen. These leaves were freeze dried using a Lyph-Lock 6 Freeze Dry System (Labconco, Kansas City, MO USA) and homogenized through grinding in a mortar in pestle with liquid nitrogen. One mg sub-samples of the leaves were packed in tin capsules and sent to University of British Columbia, Faculty of Forestry, Stable Isotope Facility for measurement of whole tissue $^{13}C/^{12}C$ isotope ratio, expressed as $\delta^{13}C$.

Extraction of soluble sugars

A 50 mg sub-sample of ground leaf tissue from each sample was weighed out and placed in a capped glass test tube. To each tube 4 mL of a methanol:chloroform:distilled water solution (12:5:3 v/v/v) was added and the samples were refrigerated overnight. The following morning the samples were removed and briefly shaken on a vortex. The samples were then centrifuged for 2 minutes at 1600 rpm and the supernatant was removed with a pipette into new glass test tubes. The pellet at the bottom of each tube, containing starch, cellulose, and other insoluble plant components was discarded. To each tube of supernatant 5 mL of distilled water was added and

shaken gently by hand. The samples were then allowed to rest for 2 hours until a visual phase separation between the aqueous and the chloroform phases occurred. The top aqueous layer was removed with a pipette into a new glass test tube. The bottom chloroform layer, containing lipids, proteins and other non-aqueous plant components was discarded.

To remove the water and methanol, test tubes containing the aqueous phase were placed in a rack in a 60°C water bath and a stream of nitrogen gas over the surface of the liquid in each test tube was applied. Samples were dry within about 2 hours using this procedure. A thick, amber coloured residue remained in the glass tubes, which were stored in the refrigerator until analysis could be undertaken.

Preparation of extract for $\delta^{13}C$ analysis

The above samples were removed from refrigeration, re-dissolved in 50 µL of methanol and homogenized by mixing. A micro-syringe was used to apply the solution to a 1 cm circle of Whatman glass filter paper to make a 2-2.5 mg sub-sample. The glass filter paper was then packed in a tin capsule and sent to the University of British Columbia, Faculty of Forestry, Stable Isotope Facility for measurement of the $\delta^{13}C$ of the aqueous extracts.

Stable isotopy

Samples were analyzed on a continual flow dual analyzer coupled with an isotope ratio mass spectrometer (Isoprime Isotope Ratio Mass Spectrometer, GV Instruments, Manchester UK). The $^{13}C/^{12}C$ ratio is expressed as a δ value in parts per million (‰) with respect to the Vienna Peedee Belemnite (VPDB) according to Equation A.1 (Farquhar et al. 1989):

$$\delta^{13}C = [(^{13}C/^{12}C)_{sample} - (^{13}C/^{12}C)_{VPDB}] / (^{13}C/^{12}C)_{VPDB} \times 1000 \quad \textbf{(A.1)}$$

Equation A.2 was used to determine the net discrimination against $^{13}CO_2$ in the tissue sub-samples and/or aqueous extracts (Farquhar et al. 1989):

$$\Delta_{obs} = (\delta^{13}C_{air} - \delta^{13}C_{tissue}) / (1000 + \delta^{13}C_{air}) \times 1000 \quad \textbf{(A.2)}$$

The isotopic composition of air can vary under greenhouse conditions (Guy et al. 1986), and therefore maize was grown alongside the trees to determine the value of $\delta^{13}C_{air}$. Tissue samples from the maize were taken three times over the course of the study and analyzed in the same manner as the leaf tissue from the trees. The average $\delta^{13}C$ of the maize leaf tissue was approximately -11.49‰, which corresponded to a $\delta^{13}C_{air}$ of approximately -8.22‰ (Marino and McElroy 1991).

Calculation of g_m

The theoretical carbon isotope discrimination based on gas exchange data (Δ_i) is calculated using Equation A.3 (Evans and von Caemmerer 1996):

$$\Delta_i = a + (b-a)C_i/C_a \quad \textbf{(A.3)}$$

The variable a is the fractionation occurring due to the diffusion in air which is equal to 4.4‰ (Evans and von Caemmerer 1996). The variable b is the fractionation associated with carbon fixation by Rubisco and, to some degree, PEP carboxylase and was taken to be 29‰ (Soolanayakanahally et al. 2009). C_a is the concentration of CO_2 of the air outside the stomata and C_i is the concentration of CO_2 at the evaporative surface inside the leaf as calculated by gas exchange.

With the calculated theoretical (Δ_i) and the observed (Δ_{obs}) carbon isotope discrimination of the tissue and aqueous extracts, internal mesophyll conductance (g_m) was calculated using Equation B.4 (Warren et al. 2006):

$$g_m = (b\text{-}a)\,(A_n/C_a)/\Delta_i - \Delta_{obs} \qquad \textbf{(A.4)}$$

Statistics

Geometric mean regressions (Model II regression) were employed using the MODELII add-In for Excel. All other statistical analyses were conducted using SigmaPlot version 13.0 (Systat 2014). Model II linear regressions were performed to explore the relationship between $\delta^{13}C$ values of tissue and aqueous extracts as well as the relationship between $\delta^{13}C$ and C_i/C_a. Pearson's correlations were performed between the estimated g_m of the tissue and aqueous extracts and the g_m estimated via A-C_i curve fitting for the ♀K4×♂C family in Chapter 3.

A.3 Results and discussion

As would be expected, a strong positive correlation between the $\delta^{13}C$ of the tissue and the extracts was observed across the three families combined ($r = 0.874$, $P < 0.0001$) (Fig. A.1). Extracts were slightly depleted in ^{13}C relative to the total tissue, by ~1.6‰. Negative correlations between $\delta^{13}C$ and C_i/C_a were observed for both the tissue and extracts of the three families (Fig. A.2), consistent with the expectation that discrimination should decrease with the steepness of the air-to-leaf CO_2 diffusion gradient and the restricted access of Rubsico to free CO_2 in the bulk atmosphere (Farquhar et al. 1989). Similar correlations between tissue $\delta^{13}C$ values and C_i/C_a are quite common in the literature (e.g., Pointeau and Guy 2014, for *Populus balsamifera*). The relationship between $\delta^{13}C$ and C_i/C_a was marginally stronger for the extracts ($r = 0.493$, $P < 0.0001$) (Fig. A.2.A) than for the tissue ($r = 0.479$, $P < 0.0001$) (Fig. A.2.B).

There was no relationship between g_m calculated from $\delta^{13}C$ values of leaves ($r = 0.052$, $P = 0.854$) or their extracts ($r = 0.164$, $P = 0.560$) and LMA (not shown). This is in sharp contrast to the estimation of g_m from A-C_i curves in Chapter 3 (Fig. 3.4). Consequently, there were no significant correlations between the g_m calculated from A-C_i curve fitting (Chapter 3) and the g_m calculated from the $\delta^{13}C$ of the tissue ($r = -0.147$, $P = 0.586$) (Fig. A.3.A) and extracts ($r = -0.024$, $P = 0.929$) (Fig. A.3.B). A lack of congruence suggests that one (or both) of the techniques employed was not successful in determining actual g_m. The stable isotope method I used here is most suspect due to the lack of relationship with LMA. There are, however, other reasons for rejecting this approach: 1. the extracts, and certainly the total leaf tissue, contained hydrophilic substances other than recent photosynthate that were acquired well before gas exchange measurements were taken; 2. possible changes in the isotopic composition of the aqueous fraction, due to the potential variation in carbon partitioning (e.g., between aqueous and

non-aqueous phases), cannot be accounted for; and 3. the isotopic signature of the CO_2 used in the LI-6400 was not close to the isotopic composition of air, possibly affecting the isotopic composition of the aqueous pool.

A.4 Conclusion

There is no correspondence between g_m calculated from the isotopic composition of aqueous extracts and g_m estimated by A-C_i curve fitting. Results from this attempt to measure internal mesophyll conductance using tissue/extract analysis to obtain carbon isotope discrimination suggest that these methods are not appropriate for estimating g_m as they stand.

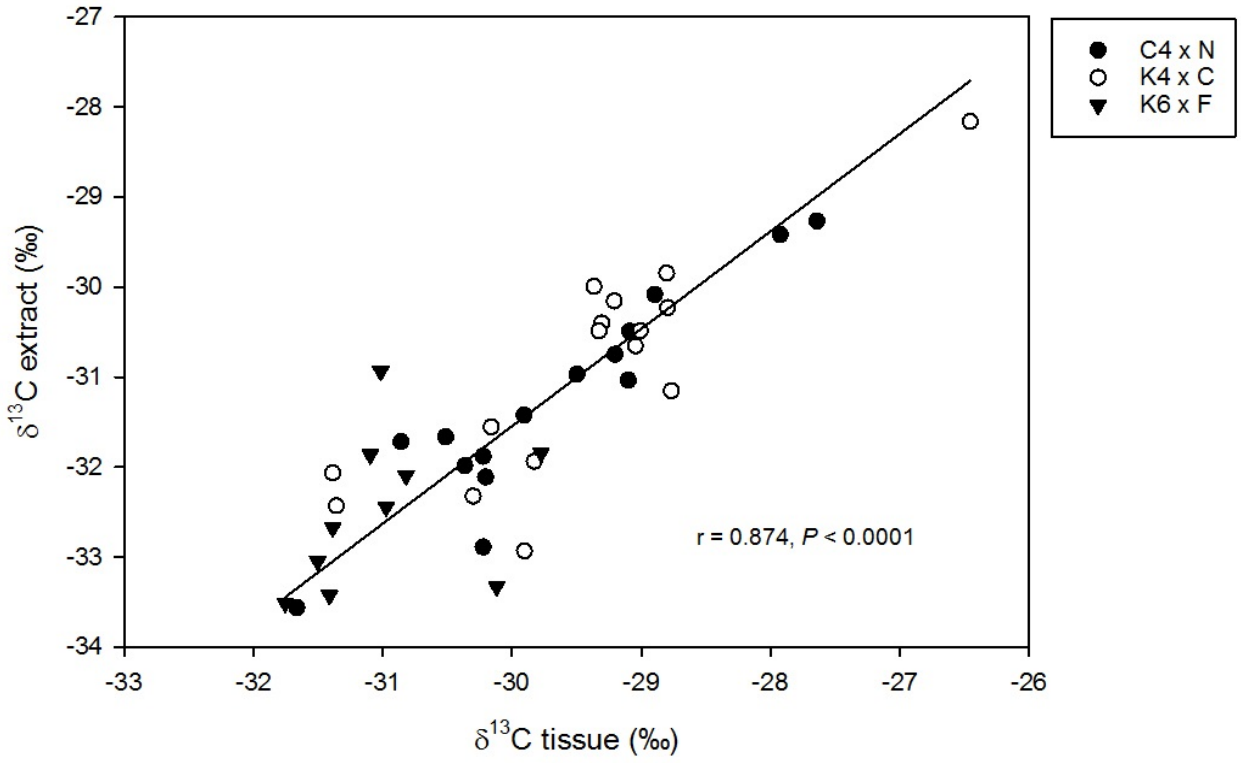

Figure A1. Relationship between $\delta^{13}C$ (‰) of aqueous extracts and that of the ground tissue of the selected three families of F_1 crosses.

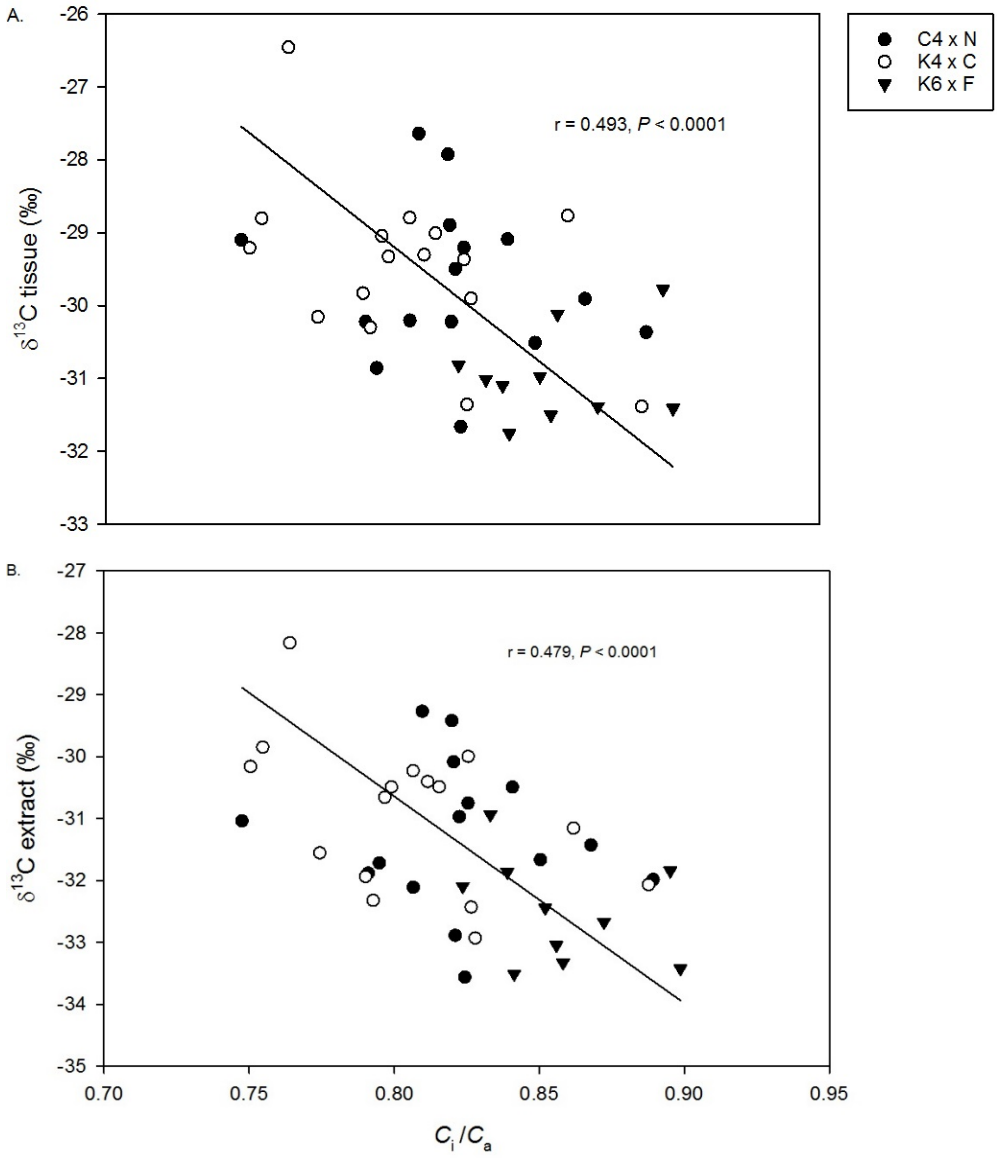

Figure A2. The relationship between $\delta^{13}C$ of tissue (A) and aqueous extracts (B) with C_i/C_a calculated from gas exchange measurements conducted in Chapter 2 of the three F_1 families.

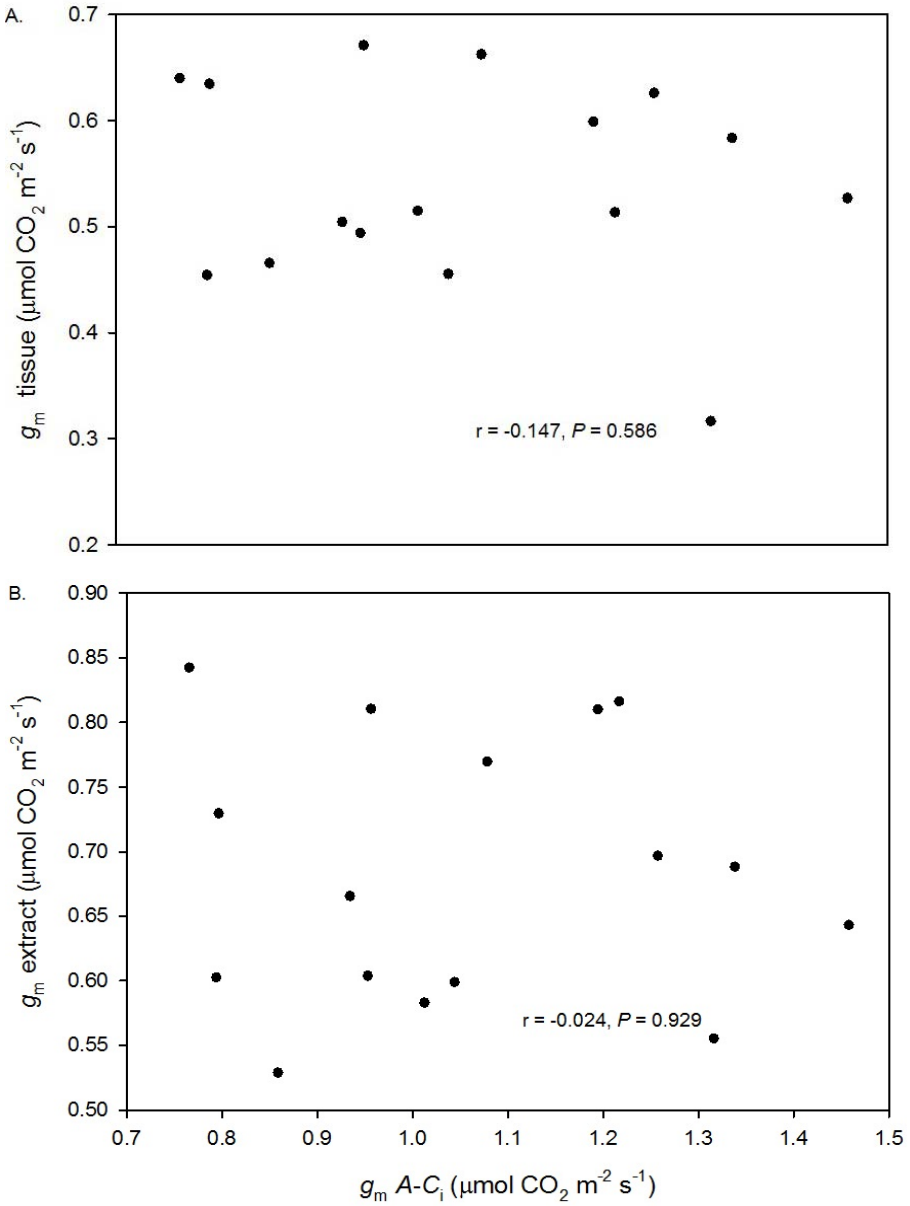

Figure A3. The relationship between the internal mesophyll conductance (g_m) estimated from ground tissue (A) and aqueous extracts (B) with the g_m estimated from the A-C_i curve fitting of the ♀K4×♂C family.